NAVAL POSTGRADUATE SCHOOL

MONTEREY, CALIFORNIA

THESIS

INVESTIGATION AND DEVELOPMENT OF OIL-INJECTION NOZZLES FOR HIGH-CYCLE FATIGUE ROTOR SPIN TEST

by

Oscar Ray Moreno

March 2005

Thesis Advisor:	Raymond Shreeve
Second Reader:	Garth Hobson

THIS PAGE INTENTIONALLY LEFT BLANK

REPORT DOCUMENTATION PAGE			Form Approved OMB No. 0704-0188
Public reporting burden for this collection of information is estimated to average 1 hour per response, including the time for reviewing instruction, searching existing data sources, gathering and maintaining the data needed, and completing and reviewing the collection of information. Send comments regarding this burden estimate or any other aspect of this collection of information, including suggestions for reducing this burden, to Washington headquarters Services, Directorate for Information Operations and Reports, 1215 Jefferson Davis Highway, Suite 1204, Arlington, VA 22202-4302, and to the Office of Management and Budget, Paperwork Reduction Project (0704-0188) Washington DC 20503.			
1. AGENCY USE ONLY ***(Leave blank)***	**2. REPORT DATE** March 2005	**3. REPORT TYPE AND DATES COVERED** Master's Thesis	
4. TITLE AND SUBTITLE: Injection and Development of Oil-Injection Nozzles for High-Cycle Fatigue Rotor Spin Test			**5. FUNDING NUMBERS**
6. AUTHOR(S) Oscar Ray Moreno			
7. PERFORMING ORGANIZATION NAME(S) AND ADDRESS(ES) Naval Postgraduate School Monterey, CA 93943-5000			**8. PERFORMING ORGANIZATION REPORT NUMBER**
9. SPONSORING /MONITORING AGENCY NAME(S) AND ADDRESS(ES) N/A			**10. SPONSORING/MONITORING AGENCY REPORT NUMBER**
11. SUPPLEMENTARY NOTES The views expressed in this thesis are those of the author and do not reflect the official policy or position of the Department of Defense or the U.S. Government.			
12a. DISTRIBUTION / AVAILABILITY STATEMENT Approved for public release: distribution unlimited.			**12b. DISTRIBUTION CODE**

13. ABSTRACT (maximum 200 words)

Resonant excitation tests of rotor blades in vacuum spin pits using discrete oil jets showed that impact erosion of the blades could limit test times, but lower excitation amplitudes were produced using mist nozzles. Smaller diameter discrete jets might extend test times, but to fully prevent erosion, oil mist droplet size needed to be 30 microns or less. The present study examined both approaches. Prototype nozzles were developed to create 0.005 inch diameter multiple discrete jets using first alumina, then stainless steel tubing, laser and micro-machine drilling. The latter technique was selected and 50 were manufactured for evaluation in HCF spin tests. A vacuum test chamber was built to observe and photograph spray patterns from the prototype nozzles and from commercially available mist nozzles. An LDV system was used successfully to determine the velocity of the oil droplets within the mist. A complete mapping of mist nozzle sprays is required to allow routine design of blade excitation systems.

14. SUBJECT TERMS High Cycle Fatigue, Laser drilled holes, Micro-drilled holes, Mist nozzles, Discrete jet nozzles, Laser Doppler Velocimetry, Liquid impact erosion, Rotor spin test			**15. NUMBER OF PAGES** 113
			16. PRICE CODE
17. SECURITY CLASSIFICATION OF REPORT Unclassified	**18. SECURITY CLASSIFICATION OF THIS PAGE** Unclassified	**19. SECURITY CLASSIFICATION OF ABSTRACT** Unclassified	**20. LIMITATION OF ABSTRACT** UL

NSN 7540-01-280-5500 Standard Form 298 (Rev. 2-89)
Prescribed by ANSI Std. 239-18

THIS PAGE INTENTIONALLY LEFT BLANK

Approved for public release; distribution unlimited.

INVESTIGATION AND DEVELOPMENT OF OIL-INJECTION NOZZLES FOR HIGH –CYCLE FATIGUE ROTOR SPIN TEST

Oscar R. Moreno
Lieutenant, United States Navy
B.S., University of Texas at Austin, 1997

Submitted in partial fulfillment of the
requirements for the degree of

MASTER OF SCIENCE IN MECHANICAL ENGINEERING

from the

NAVAL POSTGRADUATE SCHOOL
March 2005

Author: Oscar Ray Moreno

Approved by: Dr. Raymond Shreeve
Thesis Advisor

Dr. Garth Hobson
Second Reader/Co-Advisor

Dr. Anthony Healey
Chairman, Department of Mechanical and Astronautical Engineering

THIS PAGE INTENTIONALLY LEFT BLANK

ABSTRACT

Resonant excitation tests of rotor blades in vacuum spin pits using discrete oil jets showed that impact erosion of the blades could limit test times, but lower excitation amplitudes were produced using mist nozzles. Smaller diameter discrete jets might extend test times, but to fully prevent erosion, oil mist droplet size needed to be 30 microns or less. The present study examined both approaches. Prototype nozzles were developed to create 0.005 inch diameter multiple discrete jets using first alumina, then stainless steel tubing, laser and micro-machine drilling. The latter technique was selected and 50 were manufactured for evaluation in HCF spin tests. A vacuum test chamber was built to observe and photograph spray patterns from the prototype nozzles and from commercially available mist nozzles. An LDV system was used successfully to determine the velocity of the oil droplets within the mist. A complete mapping of mist nozzle sprays is required to allow routine design of blade excitation systems.

THIS PAGE INTENTIONALLY LEFT BLANK

TABLE OF CONTENTS

THIS PAGE INTENTIONALLY LEFT BLANK

LIST OF FIGURES

THIS PAGE INTENTIONALLY LEFT BLANK

LIST OF TABLES

THIS PAGE INTENTIONALLY LEFT BLANK

ACKNOWLEDGMENTS

I would like to thank Dr Raymond Shreeve for his guidance and patience. I am grateful for the opportunity to have worked with you. It has been my pleasure. I have learned a great deal.

I would like to thank Dr Garth Hobson for showing me how to use the Laser Doppler Velocimetry. Without the use of the LDV, many questions about the mist nozzles would have remained unanswered.

I would like to thank Rick Still and John Gibson because without them my experiments could not be done. They made the test equipment better than expectation. Your understanding when I broke the test equipment and how quickly you fixed it with no complaints, so I could get back to my work. Both of you truly made working at the lab a pleasurable experience.

I would like to thank Doug Seivwright for making the schematic of the prototype nozzle that was sent to selective companies so the nozzle could be made.

I would also like to thank my wife, Dena, for her support and understanding. She did not complain when I had to work on weekends or when I came home late. She was always there for me.

THIS PAGE INTENTIONALLY LEFT BLANK

I. INTRODUCTION

The reliability of gas turbine engines has continuously improved over the years. In addition to improvements in materials and manufacturing, there has been a progressive development in the analytical prediction, test and measurement techniques used in the development of new engine components. Finite element methods to calculate stresses in high-speed rotating components have become mature, and test methods to verify low-cycle fatigue (LCF) life in vacuum spin tests have become routine. In the recent years, attention has shifted to the elimination of failures that can result from high-cycle fatigue (HCF). High cycle fatigue failures can occur because an unforeseen destructive blade resonance occurs in a new rotor design, or because a flaw in the manufacture of a blade, or from damage during machine operation, which propagates until the blade eventually fails. In the early 90's, more than 30% of military engine failures were due to HCF. Also, since new military fighter aircraft were being designed to have only a single engine, and those engines incorporated integrally-machined bladed disks ('blisks', which are highly undamped, resonant structures) rather than individual blades inserted into slots, a focused 'National Gas Turbine Engine (NTE) High Cycle Fatigue (HCF) Program' was initiated in 1996.

As a coordinated effort within the NTE/HCF program, a rotor-spin research activity was initiated at the Turbopropulsion Laboratory (TPL) at the Naval Postgraduate School (NPS) to support the Navy's rotor-spin activity at NAWC-AD Patuxent River, Maryland. Specifically, the goal at TPL was to reactivate a full-scale engine rotor spin pit facility and to develop excitation and measurement techniques required to conduct HCF testing in vacuum spin chambers. By working with full-scale rotors, the techniques would automatically transition to the Navy's test activity at Patuxent River.

Since the reactivation and plans were first reported (Ref 1), air-jet excitation (AJE), oil-jet excitation (OJE) and eddy-current excitation (ECE) techniques have been investigated at NPS and used to excite a number of different rotors, including military engine turbines and fans. Strain gauge and non-contact 'time-of-arrival' blade response measurements (Ref 2) have been made, and progress has been reported at successive

NTE/HCF meetings (Ref 3-6). At the outset of the present work, it had become accepted that the only excitation technique that could be used to generate unsteady stress amplitudes which were sufficiently large, for a period of time that was sufficiently long, to prove HCF life, was the OJE technique. The OJE technique was originally proposed in Ref 1, and subsequently developed by Test Devices Inc., sponsored by the Air Force (Ref 7). Subsequent experience at TPL showed that discrete jets of oil could be used only for short periods of time without causing erosion, whereas commercial mist-producing nozzles in the same locations did not give the same high levels of blade excitation.

Therefore, the initial goal of the present study was to try to find a practical solution to the problem of erosion using discrete jets. Subsequently, when improved excitation levels were acheived in spin tests using the mist nozzles, identifying and quantifying the flow patterns produced by those nozzles became the second goal.

In the following Section II, the rotor spin pit facility is briefly described and the conclusions relating to erosion are outlined. A review of the literature related to liquid-metal impact erosion follows, and a design concept for a multi-mini-jet oil nozzle is described. In Section III, an experimental program leading to the successful development of a practical nozzle, using a windowed vacuum chamber apparatus built for that purpose, is documented. An experimental program to observe and map the flow generated by mist nozzles using a laser-Doppler velocimetry (LDV) system is described in Section IV, and conclusions and recommendations relating to both approaches are given in Section V.

II. BACKGROUND

A. ROTOR SPIN RESEARCH FACILITY AND TEST TECHNIQUE

A general view of the NPS vacuum spin pit facility in Building 215 at TPL is shown in Figure 1 and a section showing its construction is shown in Figure 2.

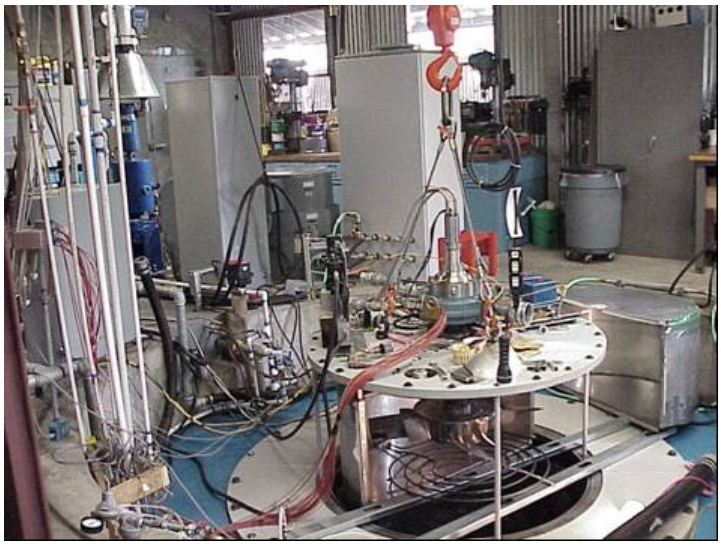

Figure 1. View of the Spin Pit Facility

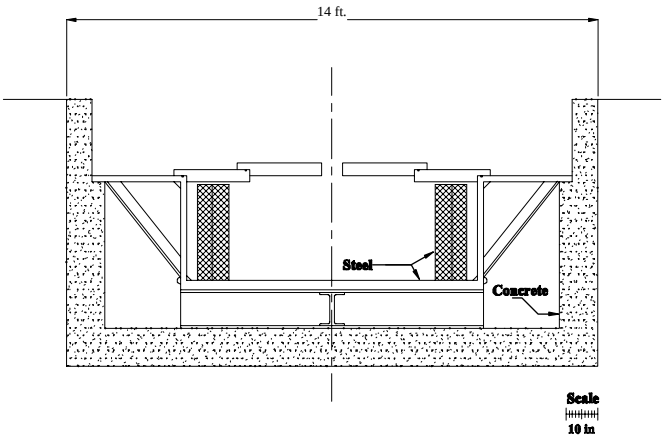

Figure 2. Section showing the construction of the pit

Test rotors are hung from a high-speed air turbine and driven up to controlled speeds in a near vacuum (typically 0.5 milli-bar). A test to measure the resonant blade response to excitation at a particular “engine-order (EO)”, where “XEO” is X times per rotor revolution, usually involves sweeping the RPM slowly through the resonant speed while

injecting through X single (or groups of) nozzles equally spaced around the periphery. The oil injection and recovery system, and arrangement of vacuum pumps, are shown schematically in Figure 3. An example of an excitation setup is shown in Figure 4. Blade response is measured using strain gages, with signals acquired through a high speed slip ring assembly attached to the turbine, which is visible in Figure 1.

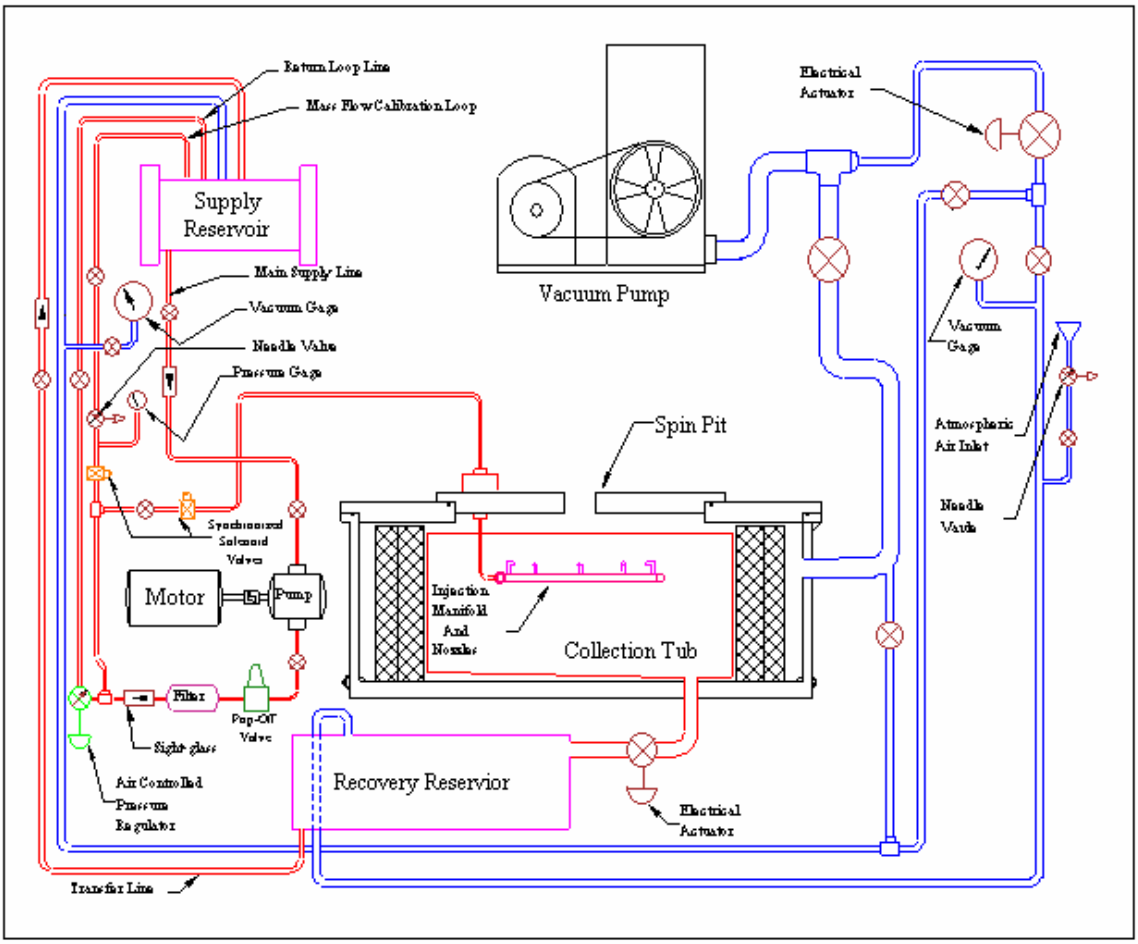

Figure 3. Schematic of oil-injection and vacuum pumping systems

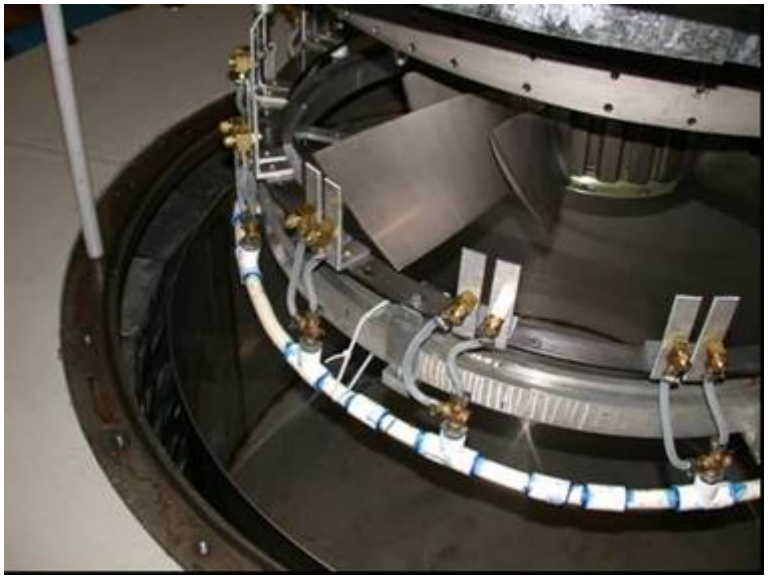

Figure 4. Oil excitation at the blade tips

B. STATUS OF OIL-JET EXCITATION DEVELOPMENT

In Reference 5, results were presented from using both discrete jets (Figure 5a) and mist-nozzles (Figure 5b) to excite resonance.

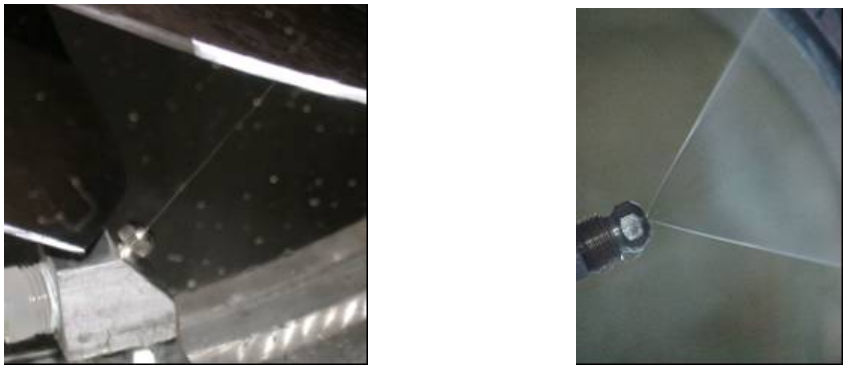

a) Discrete Jet b) Mist Nozzle

Figure 5. Discrete jet and oil mist nozzle flow patterns

However, Figures 6 and 7 (from reference 5) show that, while very high blade vibration amplitudes were achieved using discrete jets (and depended only on the mass of oil injected), erosion of the blade surface resulted after an extended exposure to oil impact.

(As can be seen in Figure 4, only a cleaning effect occurred from limited exposure). In Figure 6, the response to oil mist was clearly much lower, and therefore the challenge was to examine whether erosion was inevitable with discrete jets, or could it be avoided

by redesign; alternately, could mist nozzles be configured to give larger amplitudes. First, a review was made of the literature on impact erosion.

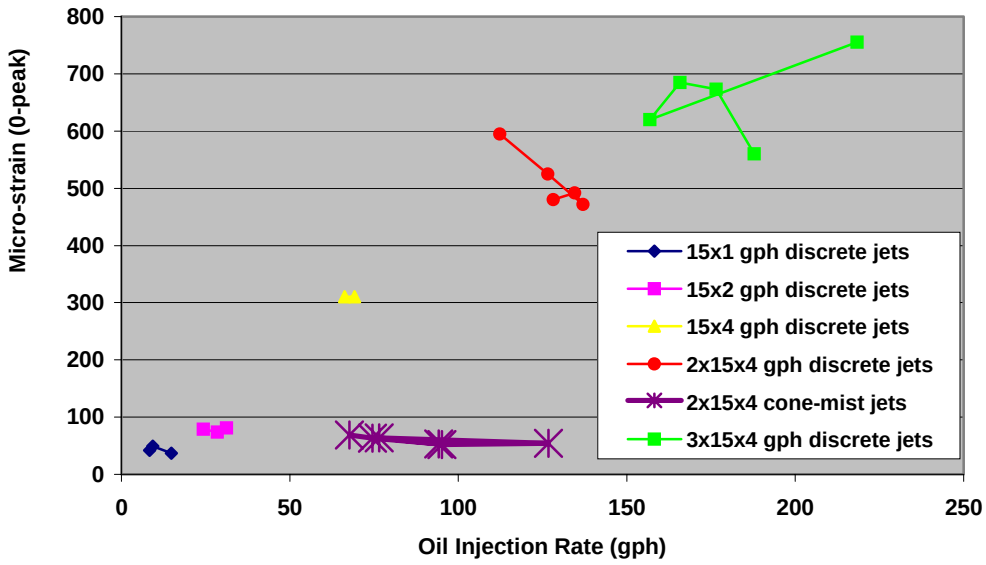

Figure 6. Amplitude of resonant response

Figure 7. Erosion of the impacted surface after extended testing

C. REVIEW OF EROSION LITERATURE

Liquid impact (or liquid impingement) erosion is the progressive loss of material from a surface due to the continued exposure to impacts [Ref 8]. The impact stream can be in the form of liquid droplets or discrete jets. This type of erosion can be found on steam turbine blades, on aircraft flying through rain, or on tubes used for heat exchangers that have bends. The erosion occurs in stages and is similar for the different types of impacts. The many factors that cause the erosion make it hard to prevent the loss of material, but there are methods to combat the erosion process and increase the life of the material.

Liquid droplets and discrete jet impacts cause erosion due to repetitive impact loads on the material. Discrete jet impacts are more severe than liquid droplets. Discrete jets impact the material along a line, so the number of impacts equals the number of impacts experienced by the target area. The damage to the material is caused by the high pressure generated at the time of the initial impact and the high velocity lateral flow of the liquid escaping from the high-pressure zone [Ref 9]. These factors are used effectively in rock and metal cutting processes. Liquid droplets do not necessarily impact the material in the same spot. The impacts can hit the material at random spots. An assumption has to be made that the drops are evenly distributed over the surface and that the area of influence of each impact is the projected area of the drop [Ref 8]. Liquid droplets cannot move at high velocities without breaking up, so the problem with liquid droplets is when a solid body moves at high velocity through an area of droplets. High contact pressure is created at each impact and causes deformation and work hardening of the surface. A water hammer effect is created [Ref 10].

Liquid impingement erosion happens in stages. The process is illustrated schematically in Figure 8. The type of impacts has no effect on whether the stages will occur, but just how long each stage lasts. The first stage is the incubation stage. During this stage, little or no material loss occurs. There is roughening and metallurgical changes are taking place on the surface. Plastic or brittle deformation in the impacted areas is also occurring. The small loss of material during this stage is attributed to weak spots on the material's surface. The incubation stage may not occur if the impacts are severe enough to immediately cause substantial material loss. During the acceleration

stage, the erosion rate increases to a maximum. Pits start to form on the surface of the material. During the maximum rate stage, the erosion remains constant. The pits grow bigger and merge to form grooves.

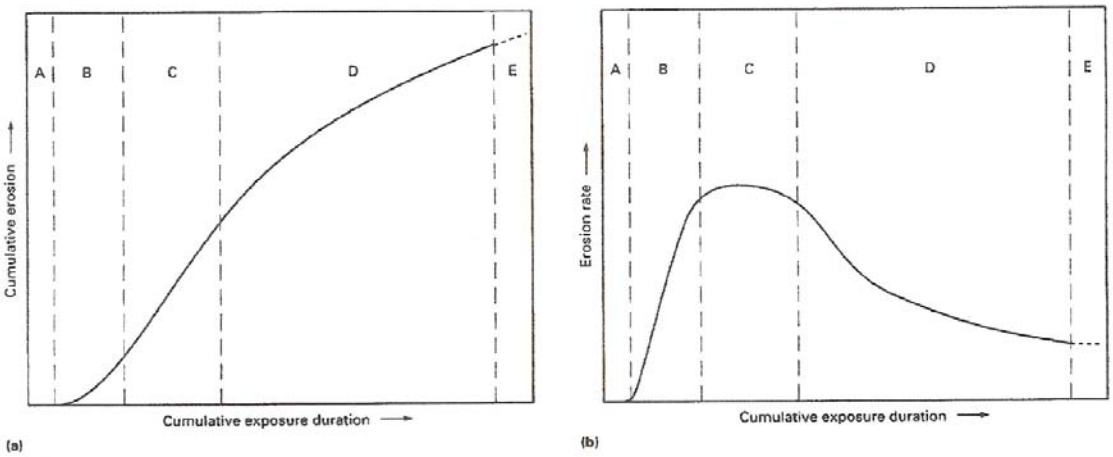

Figure 8. Characteristic erosion versus time curves. (a) Cumulative erosion versus exposure duration (time, or cumulative mass or volume of liquid impinged). (b) Instantaneous erosion rate versus exposure duration obtained by differentiating curve (a). The following stages have been identified: A incubation stage: B acceleration stage; C, maximum rate stage; D, deceleration stage, E, terminal stage. [Ref 11]

The impacted area is now covered with pits and grooves. During the deceleration stage, the erosion rate declines to approximately a half or even a quarter of the maximum erosion rate. The volume of material loss decreases because the full impact force of the liquid is no longer directly hitting the surface. The surface is uneven and possibly jagged. During the terminal stage, the erosion rate is low and continues to decrease slowly, and this is attributed to the work hardening of the material [Ref 9, 11, 12].

The cause of liquid impact erosion cannot be attributed to any one material property. The erosion is due to a combination of several properties. For liquid drop impingement, metals and alloys are eroded at stress levels that are below their respective yield strengths. Localized yielding suggests that there is non-uniformity in the strength and structure of the materials surface. The non-uniformity at the microscopic level contributes to the erosion. Thus in the incubation and acceleration stages, depressions form and grow as a result of stress concentrations caused by the change in shape of the

surface. The continued plastic deformation of the surface leads to fractures and pitting. The high speed of the liquid flowing over the surface provides the mechanism for material removal. Cavitation in the flow can cause pitting and material removal, and is another explanation for material loss [Ref 12]. Erosion in the incubation and acceleration stages is also thought to occur due to the removal of fragments caused by fatigue-like failure mechanisms. Many impacts have to occur in one area for the fragment to be loosened from the surface. The decrease in the erosion rate is harder to explain. The erosion rate decreases because the surface of the material is roughened and the surface area is increased, therefore, more energy is needed to continue the erosion. The liquid drops or jets are now impacting peaks and slopes of the roughened surface and the work hardening of the material reduces the rate of loss [Ref 12].

The way the fluid impacts the surface and magnitude of the relative velocity affects the erosion rate. If the impact velocities were low enough, the incubation period would become so long that no actual material loss would occur over a reasonable time. Erosion depends on the normal component of the impact velocity; therefore, there is an impact angle dependence. Erosion would be reduced if the impacts on the surface were more glancing [Ref 11]. The erosion rate decreases with a decrease in the droplet size. A given amount of liquid does less damage with smaller drops since there is a shorter time duration of each pressure pulse from the smaller drops. When droplet sizes were varied from 250 micrometers to 1000 micrometers, there was first an increase in the erosion rate as the droplets size increased [Ref 13]. The erosion rate peaked at 700 micrometers then decreased. The speed at which the droplets were moving affected the erosion rate. The faster the droplets were moving the higher the erosion rate. The speed did not affect the peak erosion rate at 700 micrometers. The erosion depth of the material was greater for larger droplets, but for smaller particles the erosion damage was spread over a larger area [Ref 13]. For liquid jets, the standoff distance affected the erosion rate [Ref 9]. From distances, of 2.54 centimeters to 15.24 centimeters, the material loss increased as the distance increased to a peak at 10 centimeters and then decreased. When the diameters of the jets were changed, similar results occurred. Air in the jet was thought to cause the decrease in material loss after 10 centimeters. The air reduced the erosion capability of the jet because the air acted as a cushion and changed the characteristics of the jet. The

increase in material loss to the peak standoff distance of 10 centimeters may be due to the increase of area of impingement, because of the spread of the jet [Ref 9].

To combat the erosion caused by liquid impact, the material that will be impacted by the liquid needs to be protected. A protective coating could be applied to the material, so the coating erodes and not the material. The geometry and/or fluid dynamics should be modified to reduce the amount of liquid impacting the exposed surfaces. Reducing the velocity of the droplets and the droplet size might keep the erosion rate in the incubation stage longer. The impact angles should be changed to reduce the normal component of the impact velocity. Reducing the time that the material is operating in the most severe conditions would decrease the erosion rate [Ref 14]. A combination of one or more would reduce the erosion rate and might keep the process in the incubation stage for the duration needed, or at the very least, keep it in the incubation stage for longer.

D. PROPOSED APPROACH

Clearly, from the above review, the dimension of the liquid droplets or the diameter of the impacting jets, is critical in determining the incubation period and subsequent erosion rate in any fixed arrangement of geometry and metal speed. Therefore a test chamber was built to facilitate the development of discrete jet nozzles incorporating much smaller diameter jets. The chamber subsequently allowed a variety of mist nozzles to be photographed and, in two cases, enabled a preliminary mapping to be made of the (conical) droplet velocity field.

III. VACUUM CHAMBER TEST PROGRAM

A. APPARATUS DESCRIPTION

A windowed test chamber was constructed using PVC piping, as shown in Figure 9. The chamber and associated apparatus allowed different nozzles to be tested quickly and the spray patterns to be photographically recorded at different supply pressures and flow rates.

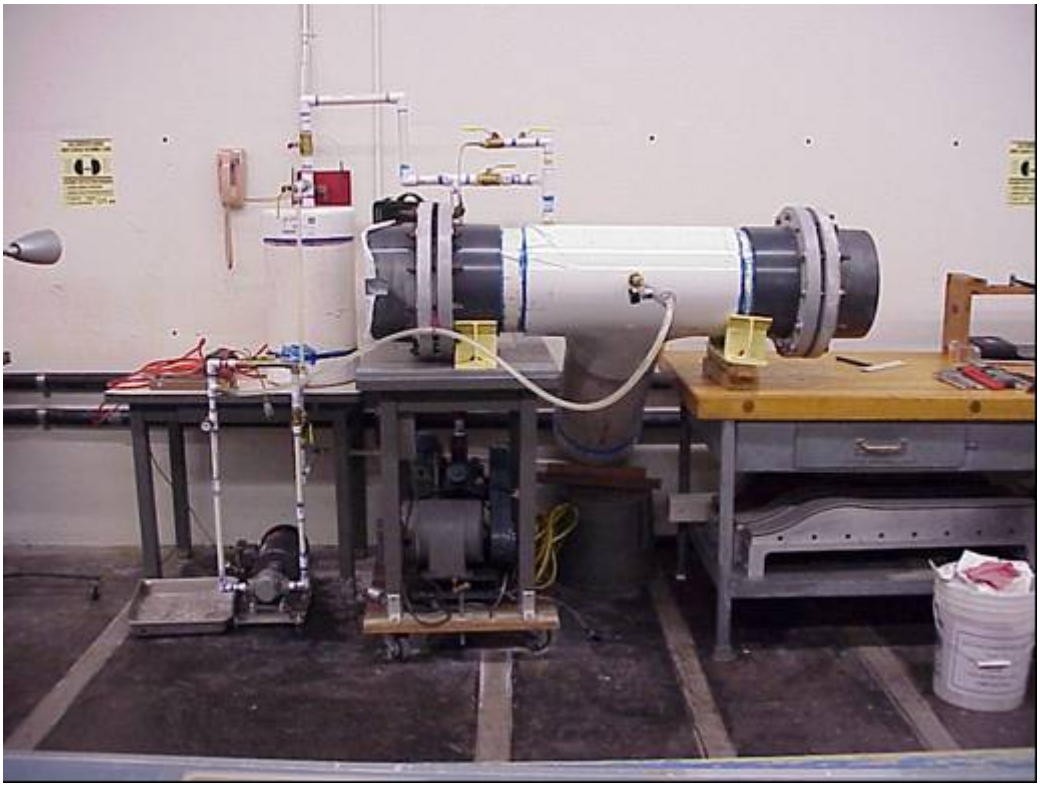

Figure 9. Oil nozzle test chamber

Details of the chamber, and the operating procedures, are given in Appendix A. The oil used throughout was MARCOL 5, made by Exxon Mobil. The Material Safety Data Sheets (MSDS) are given in Appendix B. The spray patterns were recorded using a Sony Mavica (Model MVC-DF91) digital camera. Commercial spray nozzles from various companies and prototype nozzles designed in-house were tested.

B. DISCRETE JET NOZZLE DEVELOPMENT

In an attempt to extend the erosion 'incubation period', the requirement was to develop a single nozzle that would generate multiple small-diameter discrete oil jets. For practical reasons (to maintain contamination-free oil flow using standard filters and oil pressure levels) hole diameters of 0.005 inches were to be used. Calculations predicted a flow rate of ~0.5 gph from each hole at 100 psia, so that a nozzle with 8 small holes would be equivalent to a single 4 gph nozzle with a single hole. The concept was first evaluated experimentally, using materials that were on-hand, then several different approaches to the design were pursued in parallel until a practical, cost-effective solution was found. In-house manufacture, where drilling holes as small as 0.010 was considered to be an absolute lower limit, was not an option.

The approaches that were initially considered included using metal tubing, laser drilling, electrical-discharge machining (EDM), chemical etching, and using ruby nozzles. From an internet search, using the Thomas Net directory, companies that manufacture small tubing and companies that can manufacture small diameter holes, by laser-drilling, EDM, or machine drilling were found and contacted. From these contacts, prototype nozzles were built and evaluated experimentally using the vacuum test apparatus, as described in the following paragraphs.

1. Alumina Tubing

Omega Engineering Inc. thermocouple insulators were on-hand. Nominally, the O.D. was 0.031 inches, with two 0.005 inch diameter holes. The insulator material was a brittle, glassy ceramic (alumina), and was fragile and easy to break. Examples are shown in Figure 10, against a scale divided in inches and tenths. Longer pieces were easier to handle, and this determined the method used to fabricate a nozzle. Seven intermediate lengths were bundled, epoxied together, and into a metal sleeve. When set, a grinding tool was used to cut a 0.15 inch length from the center of the bundle, which was then pressed into a hole drilled into the end of a Hago mini-mist nozzle.

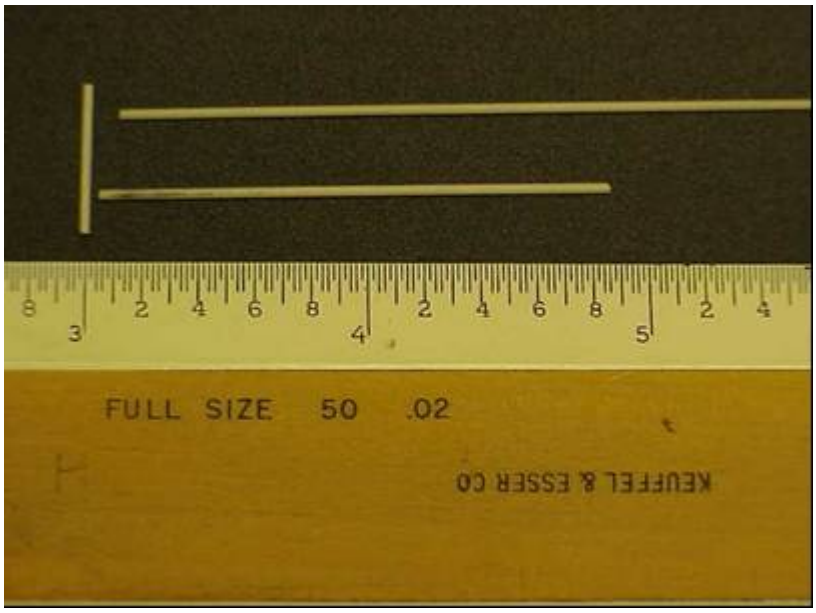

Figure 10. Ceramic tubes from Omega Engineering, Inc

The oil spray pattern obtained from the nozzle is shown in Figure 11, together with a micro-photograph of the nozzle exit surface.

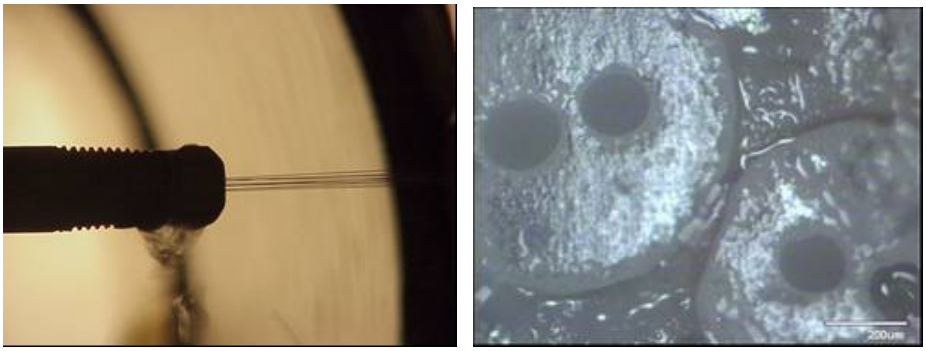

Figure 11. Alumina-Insulator nozzle flow and micro- photograph of exit surface

Since seven insulators were bundled together to make the nozzle, there should have been 14 individual jets. From the pictures taken, including rotating the nozzle to record different views, only eight discrete jets could be discerned. Since the Hago nozzles had a fine mesh filter in the inlet to the nozzle, and it was intentionally left in place when the nozzle was modified here, clogging of nearly half the holes was not to be expected. However, as can be seen in Figure 11, the holes in each insulator were extremely close to

each other (~0.002 inches) so that any two adjacent jet streams might merge into one. Another possibility is that some tubes were contaminated to begin with as a result of the grinding process used to cut the length followed by the use of shop air to clear the holes of particles.

While the test showed that oil could be supplied through a series of 0.005 inch diameter holes successfully, and insulators with only a single hole could be obtained from Omega, constructing 45 nozzles using this approach would require many man-hours, and would be unlikely to result in near-identical units.

2. Small Hole Tubes

Companies, that made hypodermic needles, which had diameters as small as 0.005 inches, were found and Vita Needles was contacted. The company could make tubes with 0.005 inch internal diameters, cut the tubes to a specified length (0.1 inch was required to limit L/D to 20 while leaving a length that could be handled conveniently), and de-burr the cut sections. Examples of the tubes are shown in Figure 12.

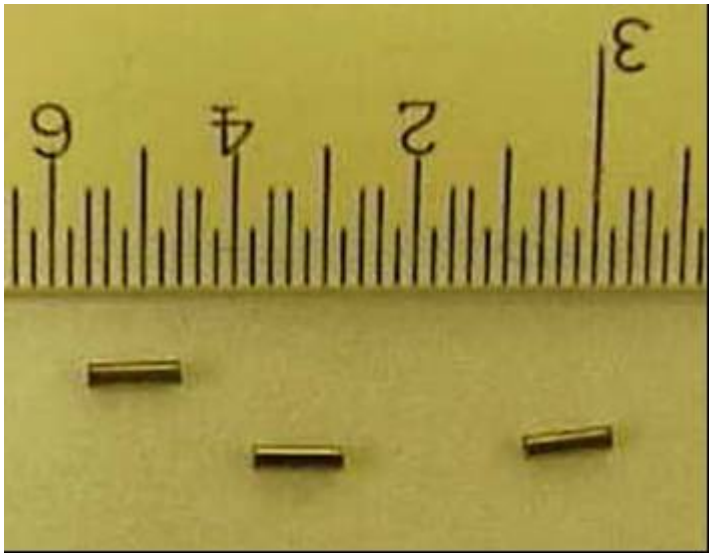

Figure 12. Tubing Sections made by Vita Needles (0.005 inch diam. by 0.1 inch long)

A test nozzle was built using a standard quarter inch pipe cap and four tube sections as shown in Figure 13. (Clearance holes were drilled into the cap and the tube

sections were inserted, using epoxy to seal). The nozzle was tested in the vacuum test apparatus and an example of the spray pattern observed is also shown in Figure 13. Four discrete jets were produced.

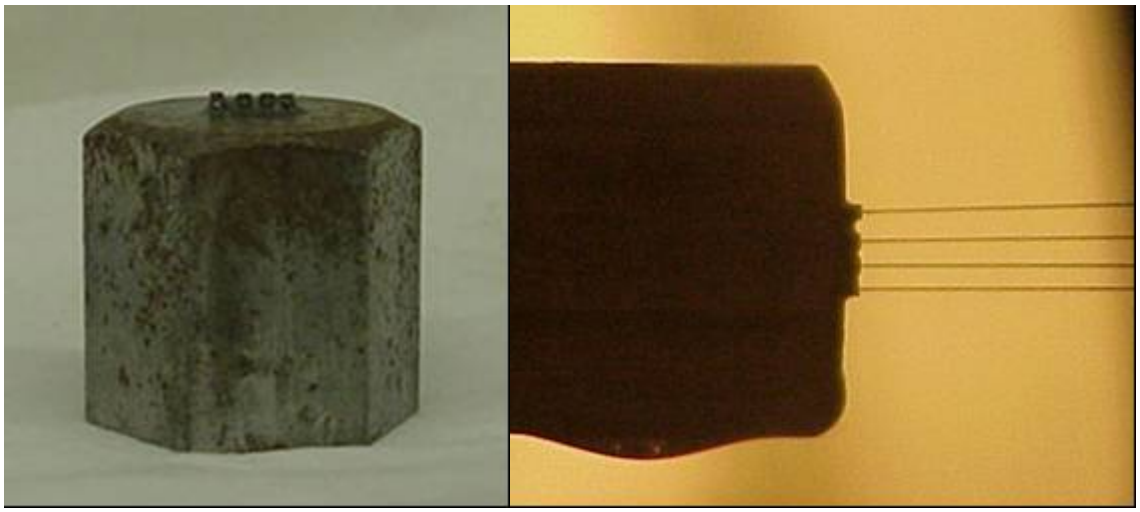

Figure 13. Prototype nozzle using tube sections from Vita Needles

The jets were near-perpendicular to the surface of the nozzle and did not interact. Though the nozzle worked successfully, it was not an economical design since it required the drilling of 0.02 inch diameter retaining holes. Creating forty-five nozzles with eight tubes in each and ensuring that the tubes were perpendicular to the surface, would be time consuming. Other options were therefore investigated.

3. Laser Drilled Holes

Laser drilling is a method that can be used to make small holes in many materials. Laser drilling is a non-contact process, so there is zero tool wear or drill breakage [Ref 15]. Laser drilling can be done by two methods: percussion or trepanning. Using the percussion drilling method, the laser beam is focused to a spot equal to the diameter of the hole to be drilled, and then either a single or several laser beam pulses are used to make the hole. The laser and the material to be drilled are held stationary during the process [Ref 16]. In the trepanning process, either the laser or the material is moved, as

the laser beam pulses are active. This is used if a larger hole is required [Ref 15]. The two most popular types of lasers used for laser drilling are the ND-YAG or CO_2 laser [Ref 17].

The ND-YAG laser is an acronym for Neodymium-Doped Yttrium-Aluminum-Garnet laser. The ND-YAG laser uses a light wavelength of 1.06 μm which can be transmitted through flexible quartz fibers. This makes the ND-YAG laser a considerably simpler design then the CO_2 lasers, and the ND-YAG laser's wavelength is absorbed more readily by metals then the CO_2 laser radiation [Ref 18]. The advantages of the ND-YAG laser are that it is a non-contact process, it is unaffected by magnetism, it produces narrow fusion and heat-affected zones with minimal shrinkage and distortion [Ref 18].

The CO_2 laser is considered the most powerful type of industrial laser available, and it is commonly used for contour cutting and deep penetration welding [Ref 18]. The CO_2 laser has a light wavelength of 10.6 μm, and most materials absorb it. The advantages of the CO_2 laser are that there is no tool wear and additionally low heat input, so there is low distortion or warping of material being cut. Cut edges are relatively smooth and approximately perpendicular to the surface; there is a narrow heat affected zone, and difficult to cut material (such as foam rubber, and very hard material, such as ceramics), can be cut [Ref 18].

Several companies were contacted. Two companies, Lenox Laser and Rache Corporation, subsequently participated in making prototype nozzles using laser drilling, for which the specification diagram is given in Appendix C.

a. Lennox Laser

Lenox Laser was provided a Swagelok SS-4-CP 316 SS pipe cap as shown in Figure 14. The inside of the pipe cap was milled (in-house) so that the top of the pipe cap was precisely uniform and 0.01 inch thick. Lenox Laser then used a ND-YAG laser to drill eight holes with 0.005 inch diameters at 0.020 inch intervals. A magnification of the surface of the resulting nozzle at 48X magnification (showing only holes 4, 5, and 6) is shown in Figure 15. The nozzle was marked to ensure that each hole could be

identified when put under the microscope again. The prototype nozzle was tested in the vacuum test apparatus. The supply pressure to the nozzle was varied from 10 psig to 150 psig.

Figure 14. Swagelok SS-4-Cp 316 pipe cap

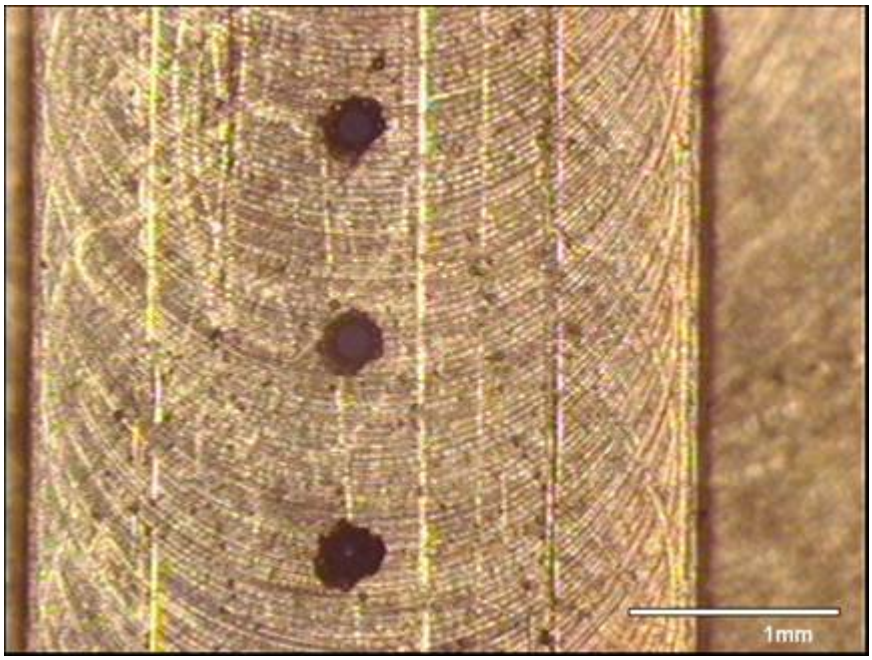

Figure 15. Lennox Laser nozzle [Holes 4(bottom), 5, and 6 at 48X magnification]

The oil spray of the nozzle at a flow rate of 100 psig can be seen in Figure 16. The individual jets were not all perpendicular to the surface of the pipe cap. Two of the jets merged to form one stream. The test was run several times to determine if small particles were clogging the holes and causing the streams to merge. The nozzle was cleaned and an extra filter was used. Similar results to that shown in Figure 16 were obtained. The holes were examined carefully again at higher magnification. It was found that the holes (on average) were about 0.01 inch in diameter and not 0.005 inch in diameter. The holes were again examined under the optical microscope, but with greater magnification.

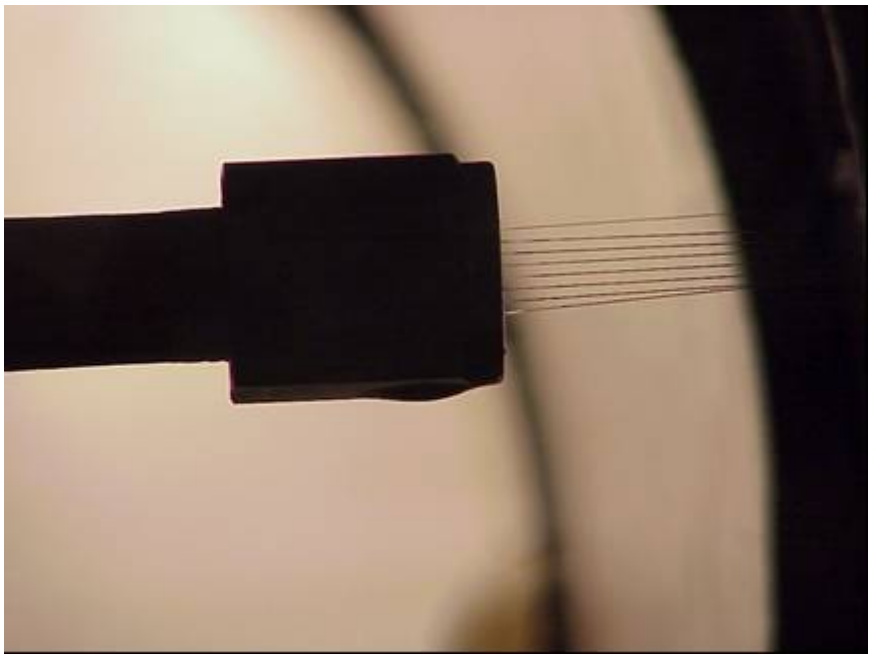

Figure 16. Lennox Laser nozzle at a flow rate of 100 psig and vacuum of 100 microns

A magnification of 290X was used and an example of the result is shown in Figure 17. The increase in magnification allowed only one hole to be examined at a time. A light was used to get a better look inside the holes at 290X magnification and the result is shown in Figure 18.

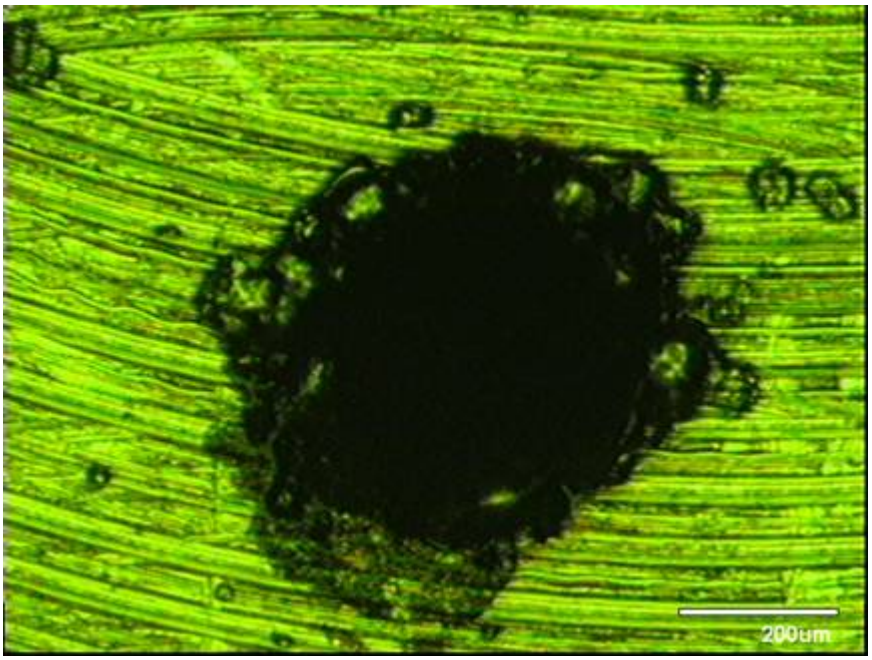

Figure 17. Lennox Laser nozzle [Hole 6 at 290X magnification]

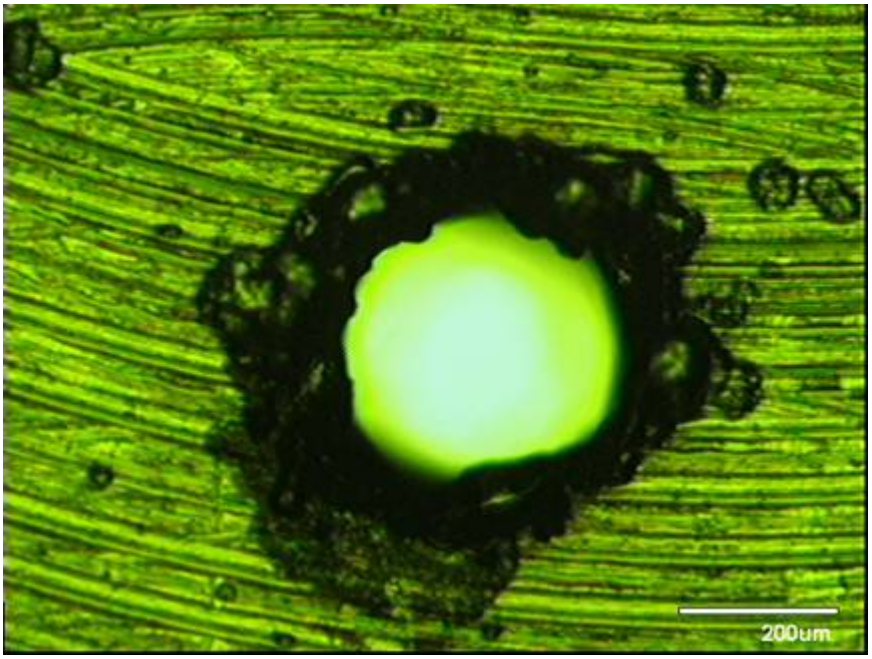

Figure 18. Lennox Laser nozzle [Hole 6 at 290X, with back lighting]

It can be seen that the hole was not round and that the surface of the hole, which is the exit, was bigger than the entrance. This was thought to play a part in causing the oil jets to not be perpendicular to the surface of the pipe cap (the oil would be exiting through an

irregular diffuser). Examination of the other 7 holes revealed that they had the same general characteristics as hole 6. Lenox Laser was contacted and it was determined that the results were the best that the company could do with their normal production methods.

b. Rache Corporation

The Rache Corporation was willing to discuss the requirements, and to suggest design changes which would achieve what was needed, using techniques that they had available. They not only did laser drilling but also welding. Therefore it was possible to first machine through the Swagelok pipe cap, and then weld a 0.01 inches thick plate on the end after the holes had been made in the plate. The plate would be attached such that the side from which the laser made the holes would be the entrance for the oil, so that the non-uniform passage would converge in area to the exit plane. The Rache Corporation made two nozzles. Both nozzles were looked at under the optical microscope at 48X magnification. Nozzle 1 is shown in Figure 19 and Nozzle 2 is shown in Figure 20. One obvious observation looking at the pictures was that the holes were smaller than the Lenox Laser holes. The holes were also examined at 290X magnification. Nozzle 1 is shown in Figure 21 and 22, and Nozzle 2 is shown in Figure 23 and 24.

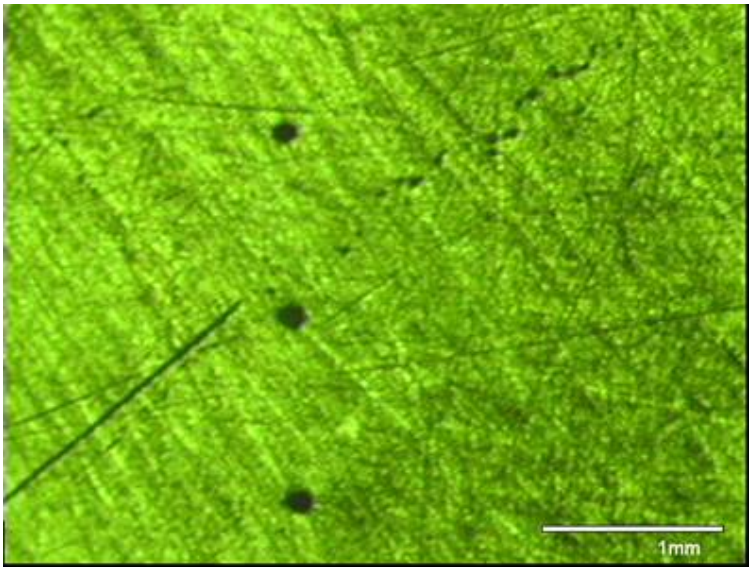

Figure 19. Rache nozzle 1 [Holes 4 (top), 5, and 6 at 48X magnification]

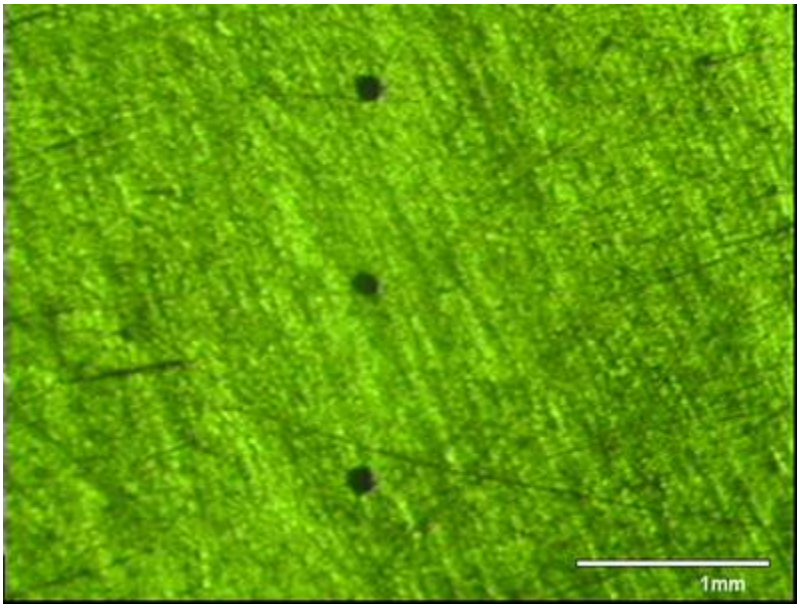

Figure 20. Rache nozzle 2 [Hole 4 (top), 5, and 6 at 48X magnification]

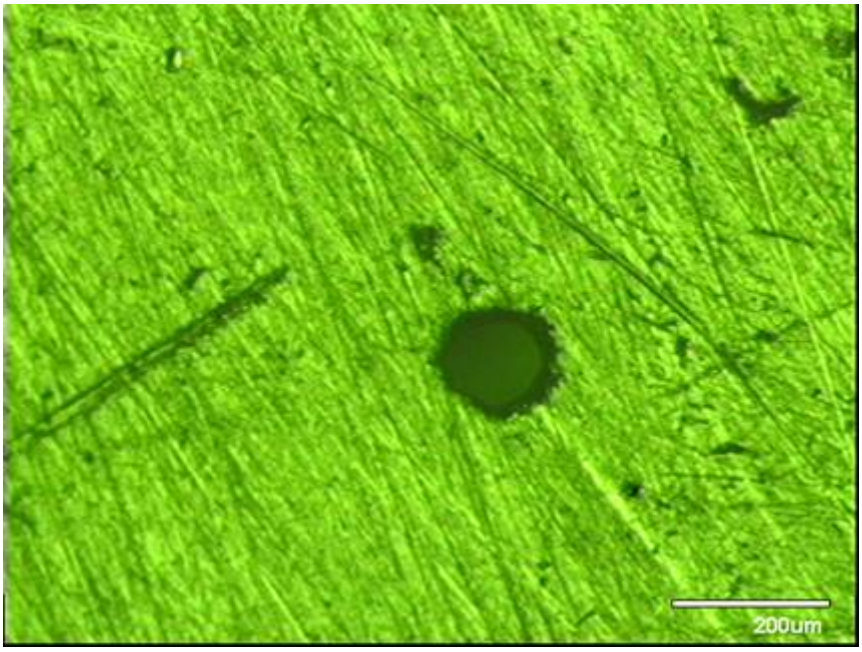

Figure 21. Rache nozzle 1 [Hole 5 at 290X magnification]

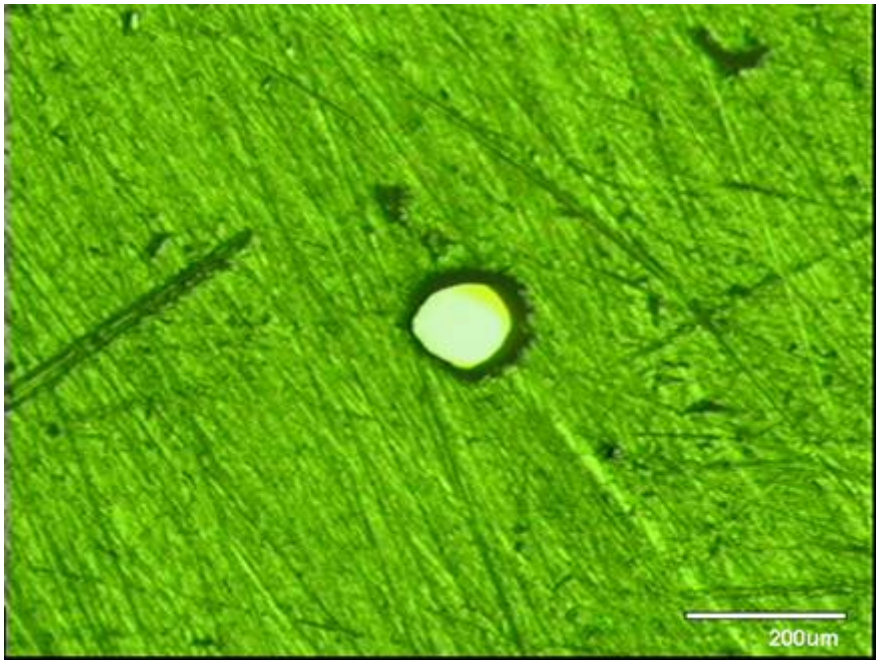

Figure 22. Rache nozzle 1 [Hole 5 at 290X, with back lighting]

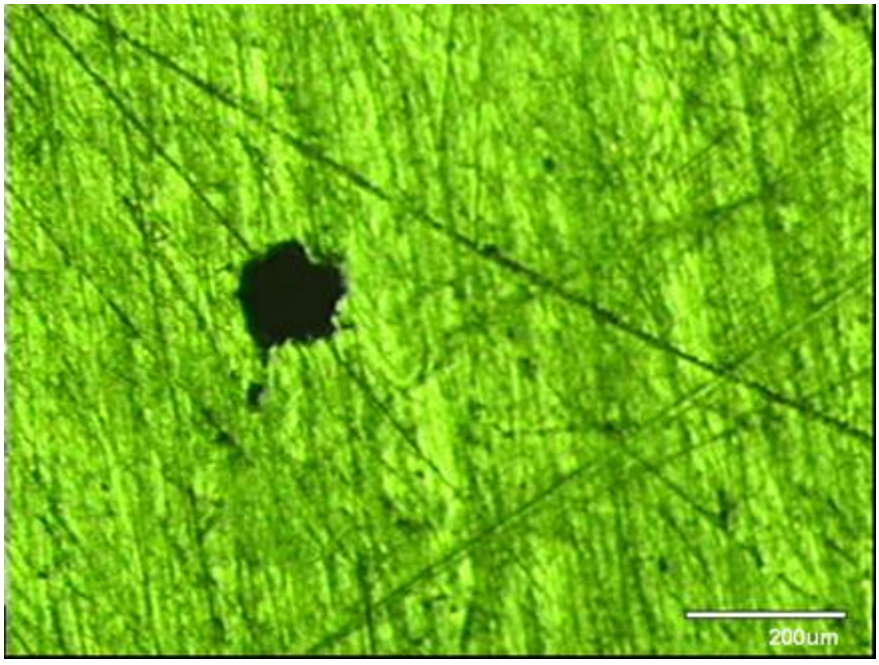

Figure 23. Rache nozzle 2 [Hole 6 at 290X magnification]

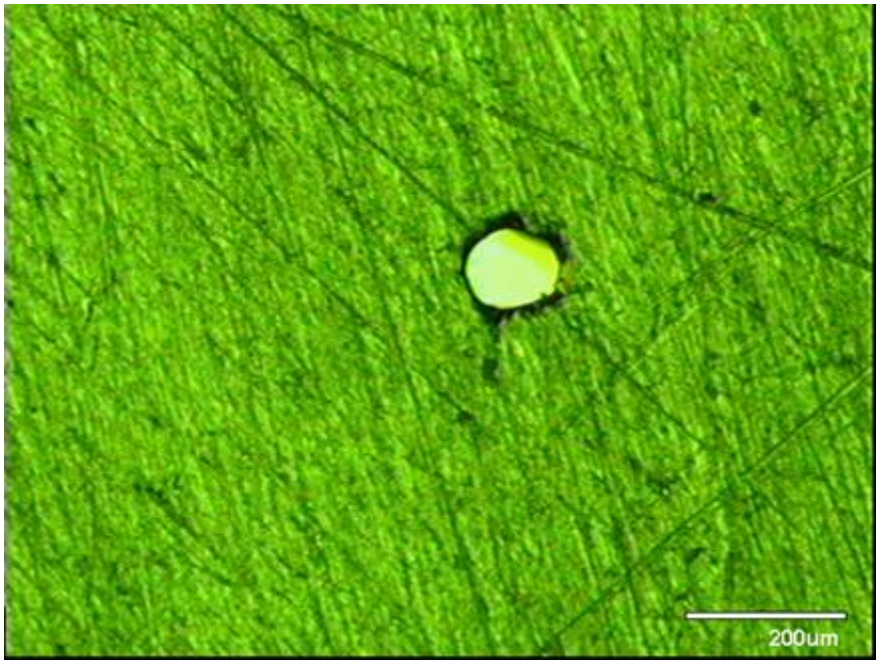

Figure 24. Rache nozzle 2 [Hole 6 at 290X, with back lighting]

The nozzles were than tested in the vacuum test chamber. The oil supply pressure was varied from 10 psig to 110 psig. The results for Nozzle 1 and Nozzle 2 at 100 psig are shown in Figure 25 and Figure 26, respectively. The spray patterns for both nozzles showed jets, which were not perpendicular to the surface of the nozzle. Since the holes in the nozzles were now smaller, a finer filter was added in the line to ensure that small particles were not clogging the holes. The spray pattern did not change. The holes were then examined under the optical microscope at 340X magnification and the results are shown in Figure 27, 28, 29 and 30. The Rache Corporation was contacted to see if the drilling process could be refined to make smoother, rounder holes, but the process they used would not allow it. Since similar results had resulted using two different companies, laser drilling was not pursued further.

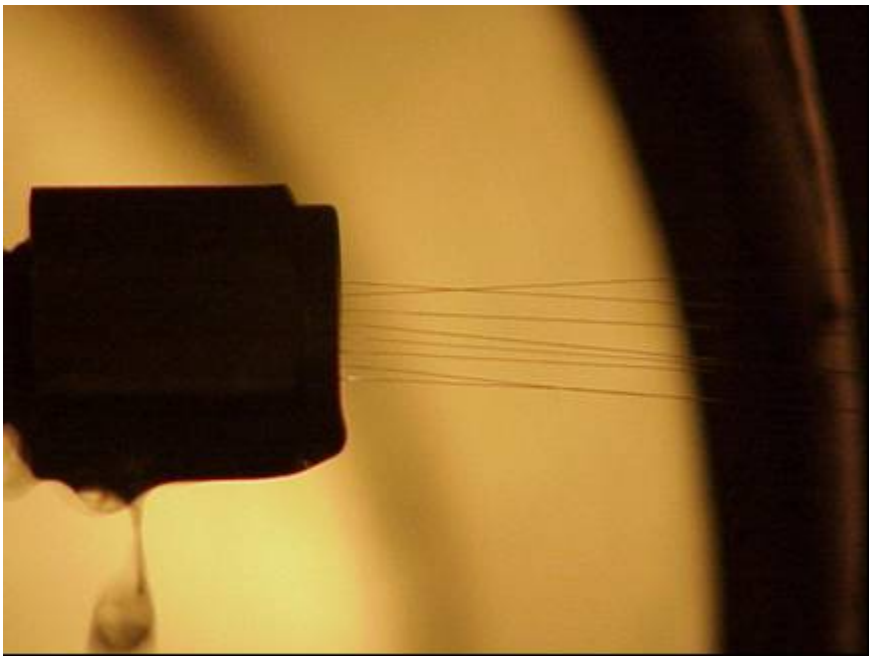

Figure 25. Rache nozzle 1 [100 psig into 150 microns]

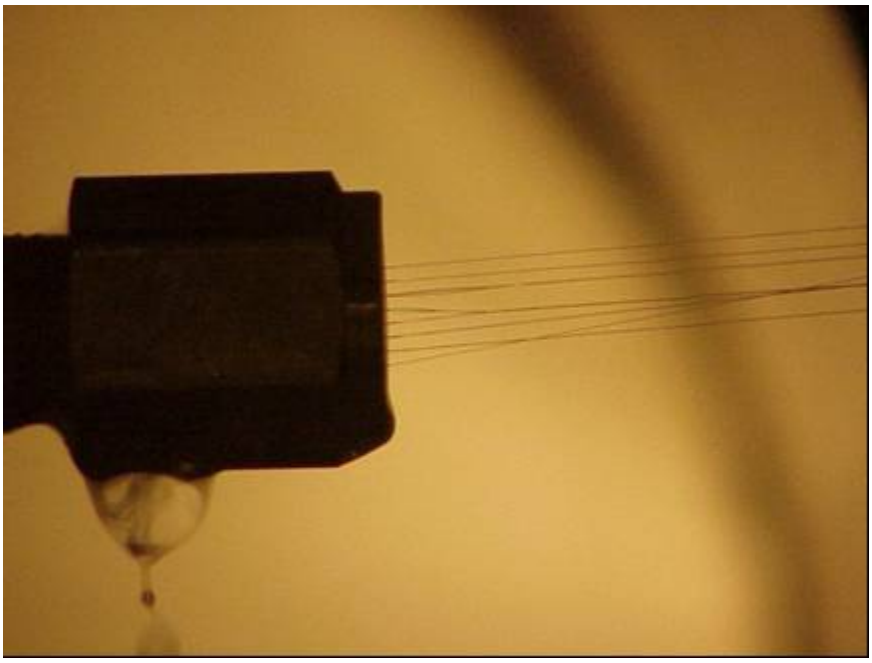

Figure 26. Rache nozzle 2 [100 psig into 150 microns]

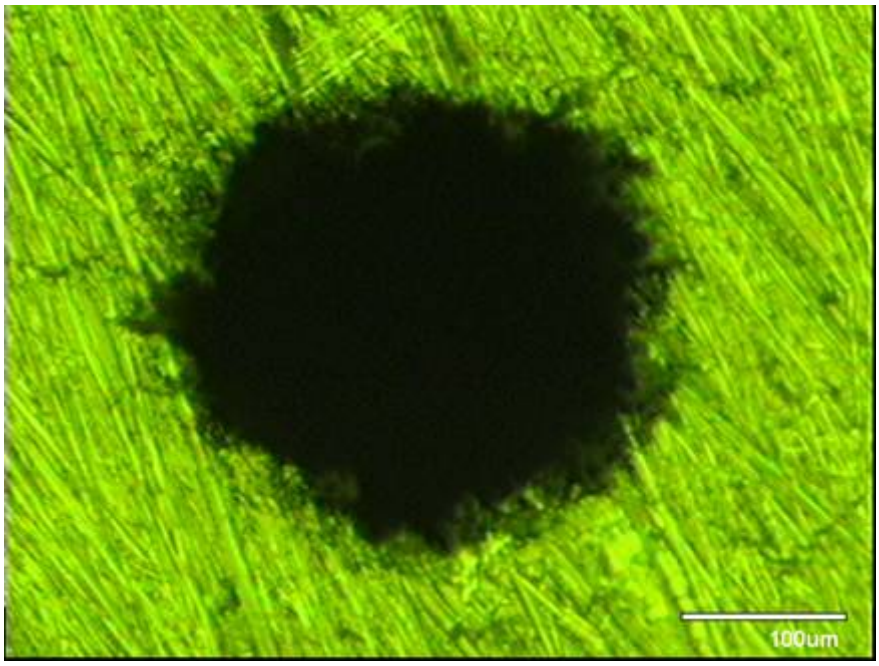

Figure 27. Rache nozzle 1 [Hole 5 at 340X magnification]

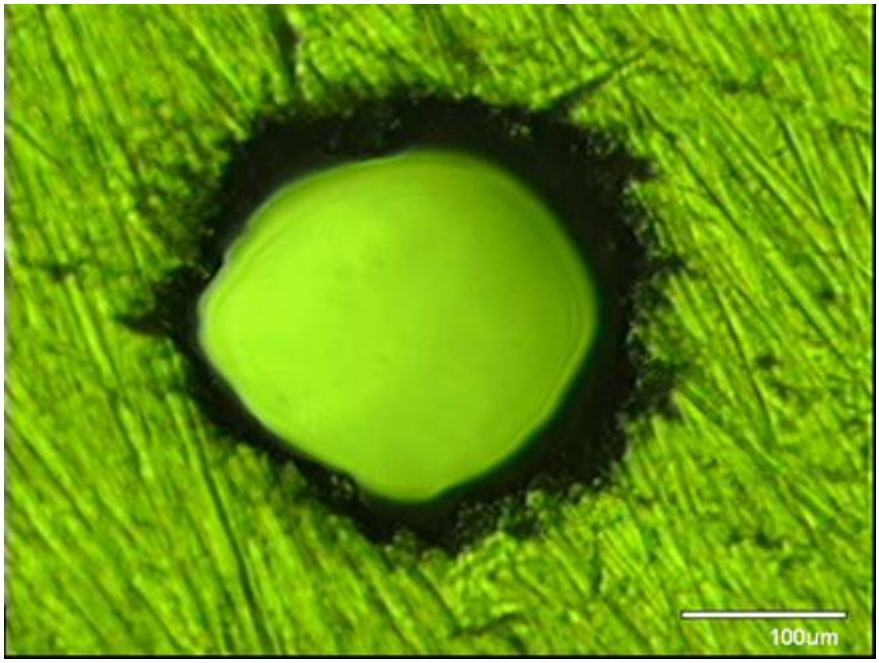

Figure 28. Rache nozzle 1 [Hole 5 at 340X, with back lighting]

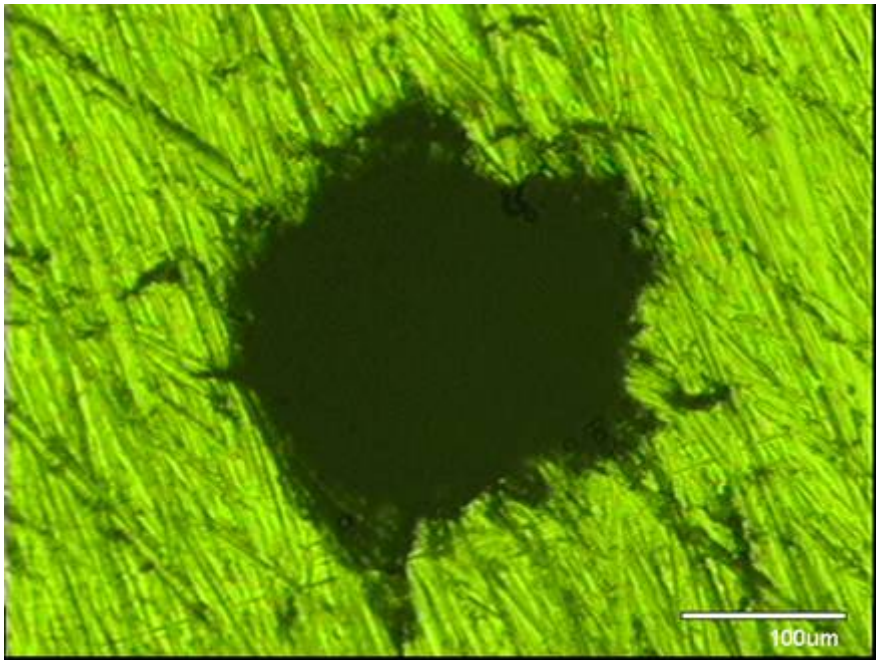

Figure 29. Rache nozzle 2 [Hole 6 at 340X magnification]

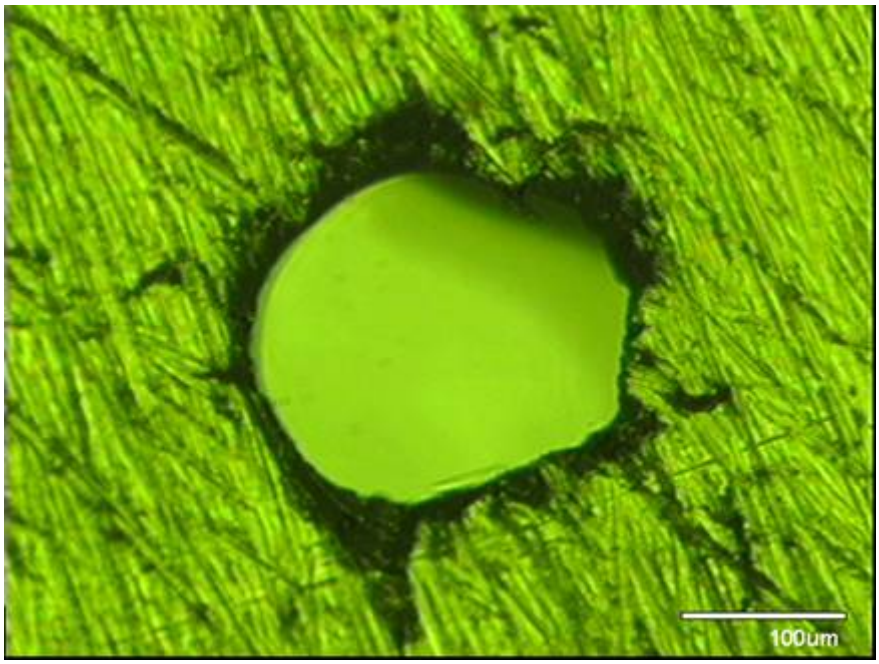

Figure 30. Rache nozzle 2 [Hole 6 at 340X, with back lighting]

4. Electrical Discharging Machining

Wire EDM uses a controlled electrical current or spark erosion to remove metal (Ref 19). During the EDM process, a series of timed electrical pulses remove material from the specimen. The specimen and an electrode are immersed in a dielectric. A power supply controls the timing and the intensity of the electrical charges (Ref 20). The electrical sparks vaporize and melt the metal and create a crater in the specimen. Each spark can reach temperatures between 8000 and 12,000 degrees Celsius (Ref 21). Particles are removed by the continuous flushing of the dielectric fluid. The electrical discharges produce micro-craters and the discharging continues until the desired shape is made (Ref 22). Companies that use wire EDM to make small holes were not asked to attempt a prototype nozzle laser since there was clearly some similarity with the laser drilling technique, and because an economical solution was found in micro-drilling.

5. Micro-drilled Holes

Most companies contacted could not machine-drill holes as small as 0.005 inches. Most were limited to 0.008 inches to 0.01 inches. However, one company, Vermont Mold & Tool, stated on their website that they could drill holes accurately down to 0.0028 inches. The company was contacted, and they offered to make a nozzle with 0.005 inches diameter holes through a surface with a thickness of 0.01 inch. A standard Swagelok pipe cap, shown in Figure 14, was sent to the company, who returned a prototype nozzle. The nozzle was put under the optical microscope at 48X magnification and the result is shown in Figure 31. The magnification was set to 290X, and the resulting pictures are shown in Figure 32 and 33. The holes were seen to be round with no jagged edges. The magnification was increased to 340X, and the result is shown in Figure 34. The nozzle was then installed in the vacuum test chamber and the oil supply pressure was changed from 10 psig to 120 psig. The spray pattern from the nozzle at a pressure of 100 psig for two different runs is shown in Figure 35 and 36. The discrete jets of oil coming out of the nozzle are seen to be perpendicular to the surface.

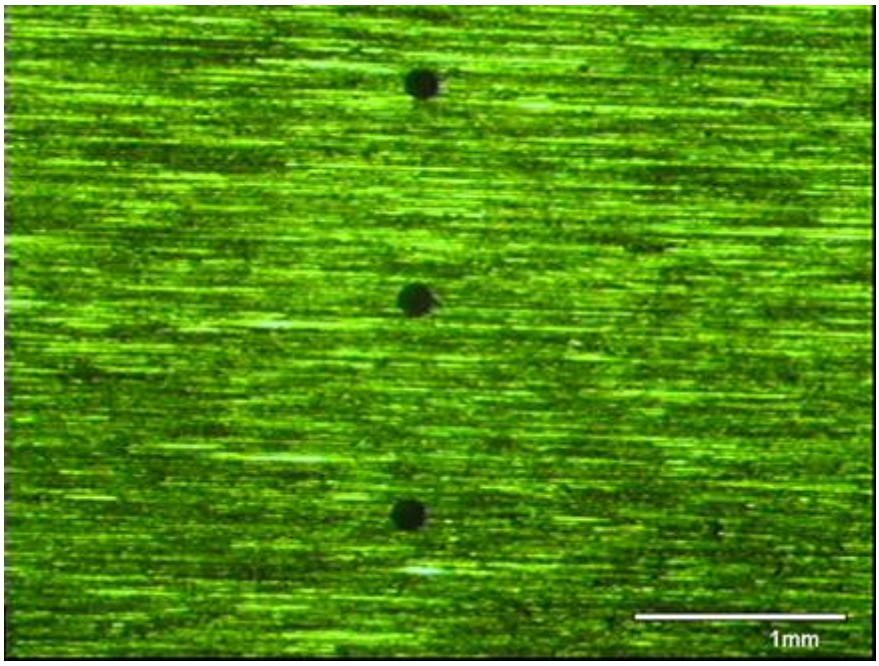

Figure 31. Vermont nozzle [Holes 4 (top), 5, and 6 at 48X magnification]

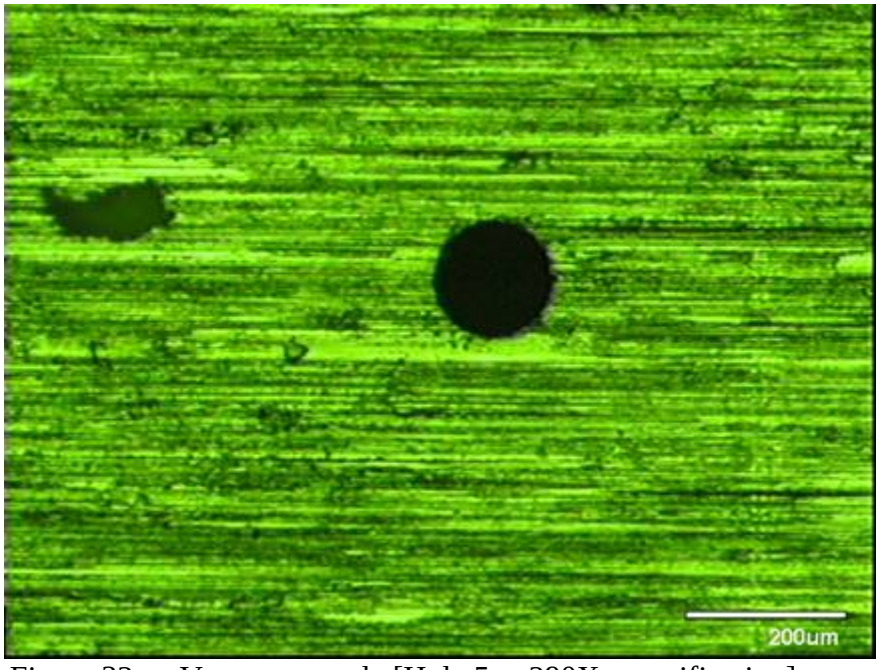

Figure 32. Vermont nozzle [Hole 5 at 290X magnification]

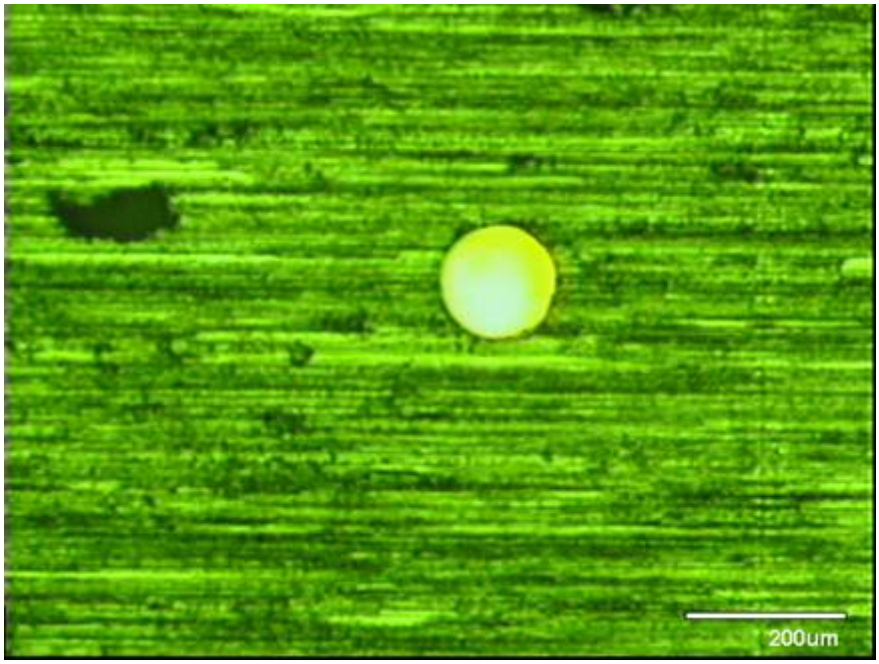

Figure 33. Vermont nozzle [Hole 5 at 290X, with back lighting]

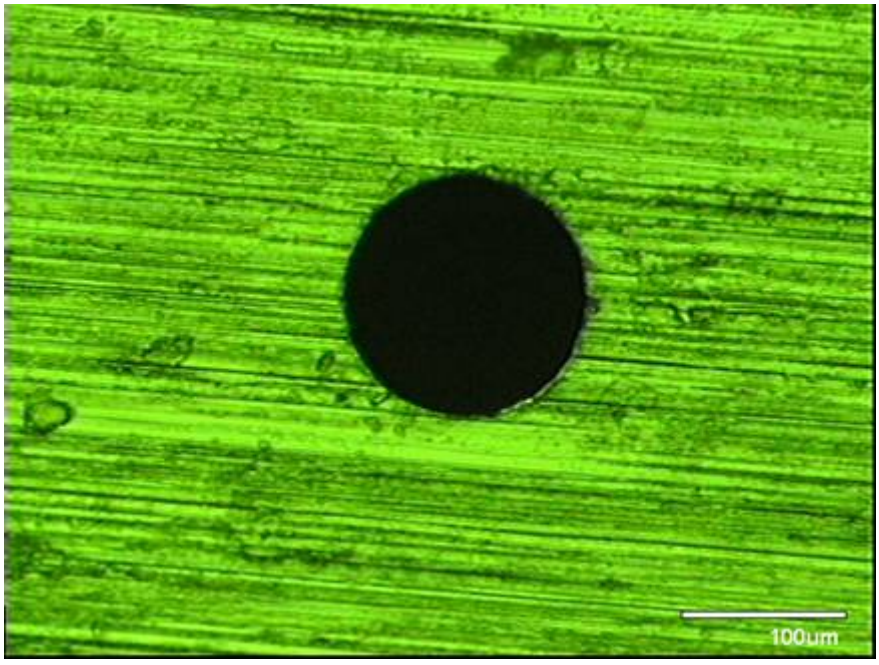

Figure 34. Vermont nozzle [Hole 5 at 340X magnification]

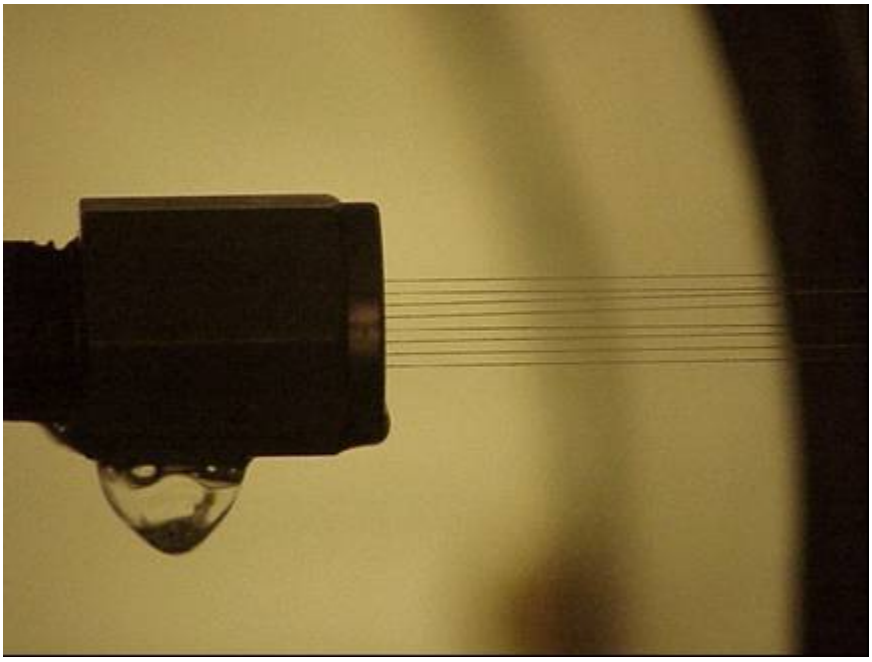

Figure 35. Vermont nozzle [100psig into 60 microns]

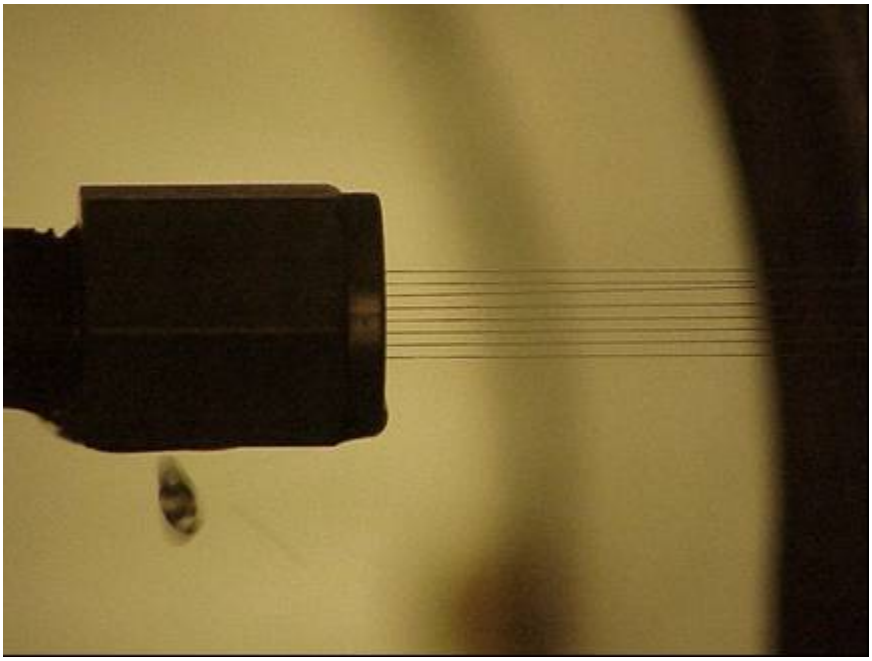

Figure 36. Vermont nozzle [100psig into 70microns]

Experience with the prototype nozzle showed that particular care was needed in handling such nozzles. To obtain perpendicular streams after attaching the nozzles to the wand required careful handling of the nozzle, and the use of micro-filters to keep the

holes clean. Filters that can filter particles much smaller than the hole diameters are needed. Nitrogen was used to blow out any particles that could clog the holes, but merely touching the surface of the nozzle could cause the nozzle to get partially blocked, and lead to an errant stream direction.

Following the series of prototype tests, it was concluded that the prototype nozzle met the required specifications. Similar nozzles (49) have since been delivered to complete a total order of fifty.

C. MIST NOZZLE SPRAY PATTERNS

Fog nozzles produce small diameter particles. If less than 30 micrometers, small particles will not erode turbine blades [Ref 7]. The spray patterns of four Hago brand nozzles of different flow capacities (rated in gallons per hour, gph]) were examined. The four nozzles tested were a 1-gph, a 2-gph and a 4-gph 'mini-mist', and a standard 6-gph nozzle. Each nozzle was installed, in turn, on the wand in the vacuum test chamber, and the oil pressure was increased from 10 psig to 120 psig. Pictures of the spray patterns from each nozzle were taken at 10 psig intervals. All tests were carried out using Exxon Marcol 5 oil. The results are described in the following paragraphs. [For scaling purposes, the hex-head of the mini-mist nozzles measured 0.44 inches and the standard nozzle 0.625 inches across the flats].

1. 1-gph Mini-Mist Nozzle

The results for the 1-gph mini-mist nozzle are shown in Figure 37 for 10-60 psig and Figure 29 for 70-120 psig. It can be seen that the nozzle did not produce a mist or a cone from 10 to 60 psig. Instead, the flow was similar to a discrete jet. The spray pattern changed when the flow pressure was over 70 psig as shown in Figure 38. The oil started to form a cone shape, but the oil clearly did not mist completely. The spray pattern contained oil streams. At the maximum test flow pressure of 120 psig, the spray pattern gave a total spray angle of about 40 degrees, compared to the manufacturer's quoted cone angle of 80 degrees.

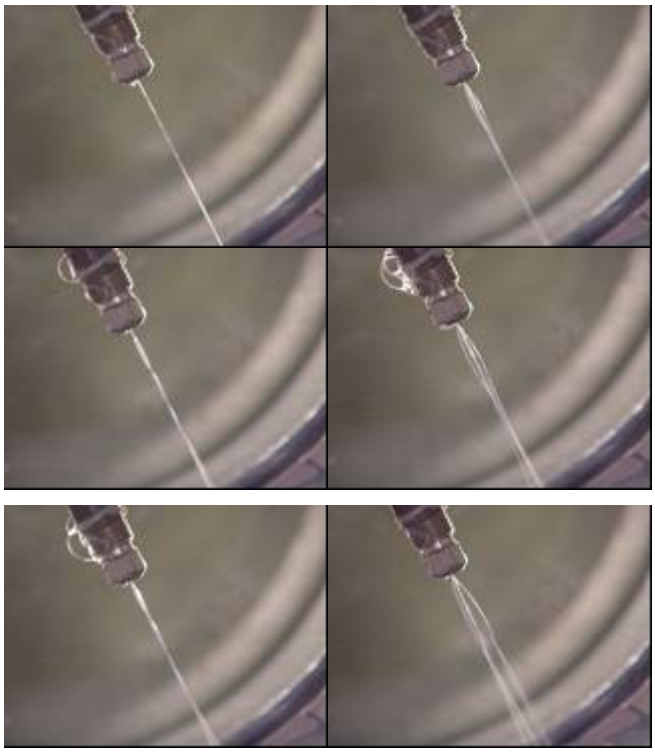

Figure 37. Hago 1-gph mini-mist nozzle: Left side, 10 (top), 20 (middle), 30 (bottom) psig. Right side, 40(top), 50 (middle), 60 (bottom) psig

Figure 38. Hago 1-gph mini-mist nozzle: Left side, 70 (top), 80 (middle), 90 (bottom) psig. Right side, 100(top), 110 (middle), 120 (bottom) psig.

2. 2-gph Mini-Mist Nozzle

The results for the 2-gph mini-mist nozzle are shown in Figure 39 for 10-60 psig and Figure 40 for 70-120 psig. It can be seen that the 2-gph nozzle did not form a mist until the flow pressure was 50 psig or greater. The spray pattern below 50 psig was not a full cone, and clearly contained liquid streams. Flow pressures greater than 50 psig caused the angle of the cone to increase only slightly, and it is clear that the oil is misting.

3. 4-gph Mini-Mist Nozzle

The results for the 4-gph mini-mist nozzle are shown in Figure 41 for 10-60 psig and Figure 42 for 70-120 psig. The pictures show that the 4-gph nozzle started to mist at about 20 psig. The cone angle increased until about 60 psig, after which it was nearly constant, and close to the manufacturer's specified 80 degrees. A mist was produced at about 20 psig and above, but it is not certain whether the mist extends back to the nozzle itself. The initial cone appeared to reflect light from the edges and was transparent through the center. Based on these observations, the 4-gph nozzles can be used in spin tests at lower pressures, but a question remains as to how close to the test blade they can be located.

4. 6-gph Standard Nozzle

The results for the 6-gph standard nozzle are shown in Figure 43 for 10-60 psig and Figure 44 for 70-120 psig. It appears that there were some streaks of liquid oil in the spray pattern at all pressures. At flow pressures greater than 50 psig, the edge of the conical spray seems to contain streaks. Since this is relevant to the question of erosion in spin tests, a second nozzle of the same type was tested, and very similar results were obtained.

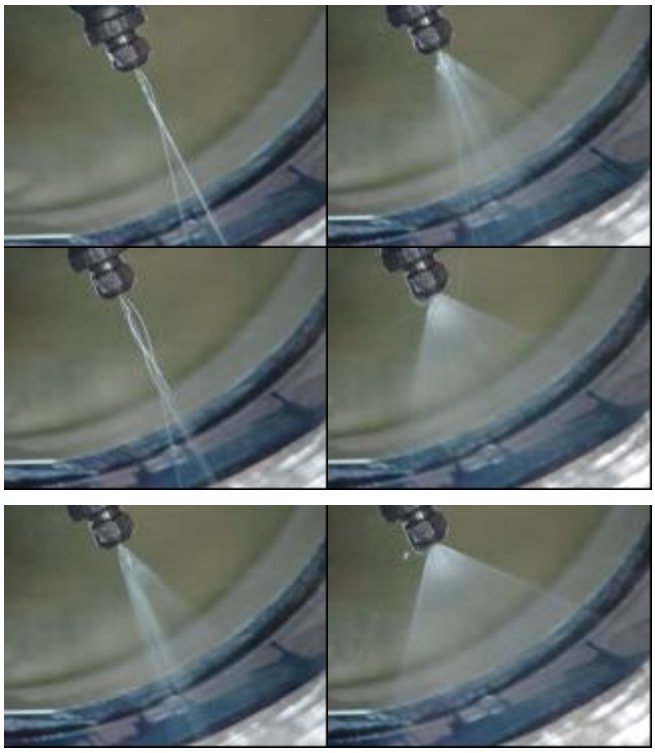

Figure 39. Hago 2-gph mini-mist nozzle: Left side, 10 (top), 20 (middle), 30 (bottom) psig. Right side, 40(top), 50 (middle), 60 (bottom) psig

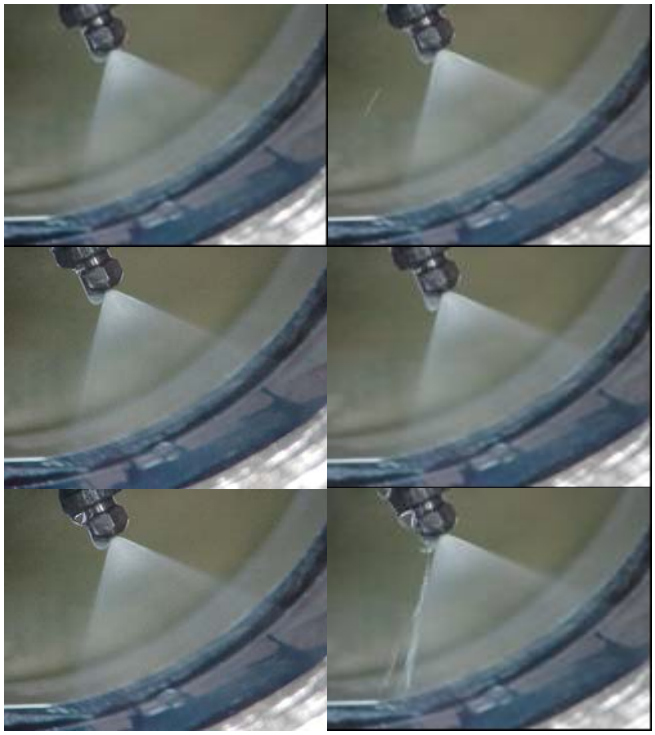

Figure 40. Hago 2-gph mini-mist nozzle: Left side, 70 (top), 80 (middle), 90 (bottom) psig. Right side, 100 (top), 110 (middle), 120 (bottom) psig

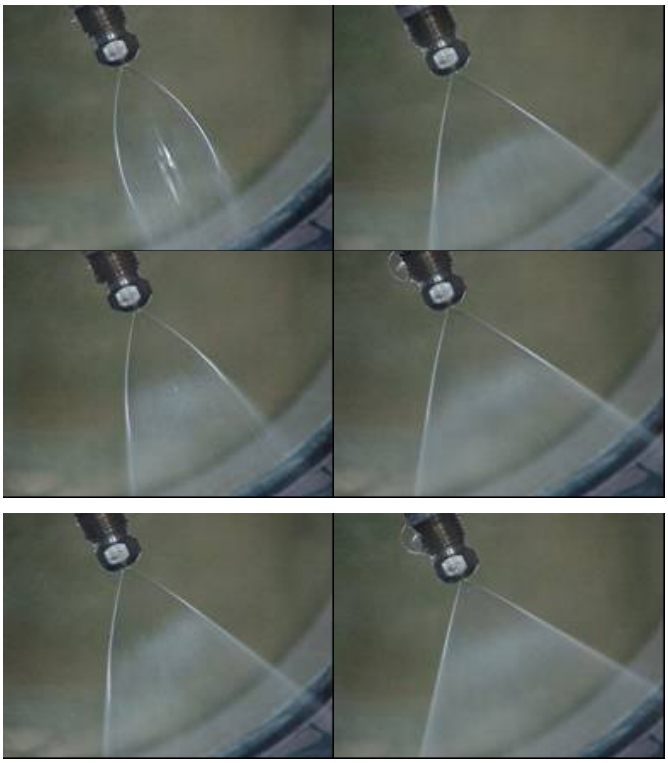

Figure 41. Hago 4-gph mini-mist nozzle: Left side, 10 (top), 20 (middle), 30 (bottom) psig. Right side, 40 (top), 50 (middle), 60 (bottom) psig.

Figure 42. Hago 4-gph mini-mist nozzle: Left side, 70 (top), 80 (middle), 90 (bottom) psig. Right side, 100 (top), 110 (middle), 120 (bottom) psig.

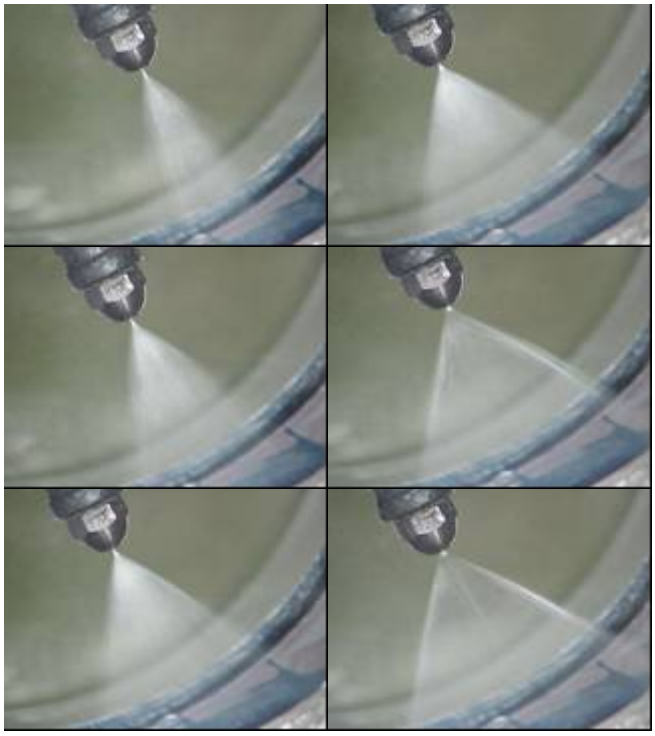

Figure 43. Hago 6-gph standard nozzle: Left side 10 (top), 20 (middle), 30 (bottom) psig. Right side, 40 (top), 50 (middle), 60 (bottom) psig.

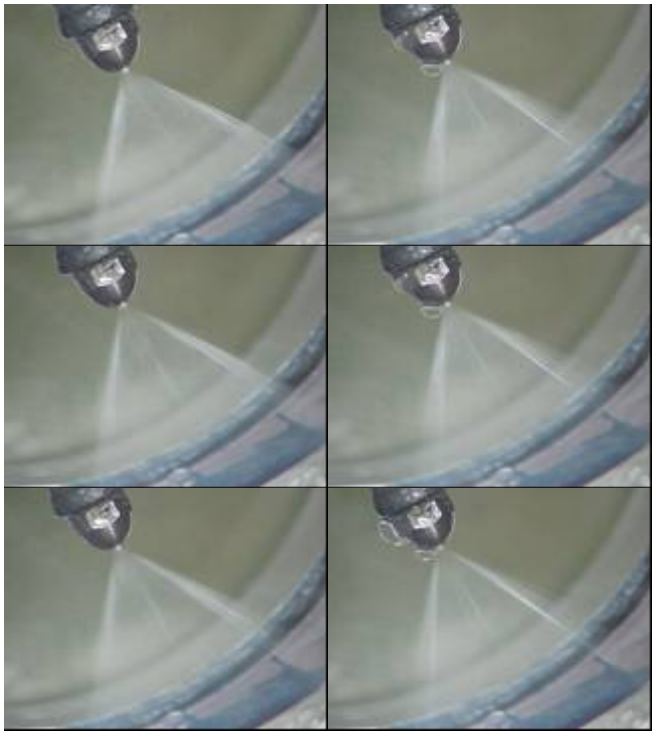

Figure 44. Hago 6-gph standard nozzle: Left side, 70 (top), 80 (middle), 90 (bottom) psig. Right side, 100 (top), 110 (middle), 120 (bottom) psig.

IV. LASER DOPPER VELOCIMETRY

A. APPARATUS DESCRIPTION

To measure the velocity of the droplets from various commercial nozzles, a Laser Doppler Velocimeter (LDV) made by TSI Incorporated was used. The LDV system and transverse mechanism can be seen in Figures 45 and 46.

Figure 45. TSI Incorporated LDV system

Figure 46. Side view of the LDV and transverse mechanism

The LDV system was used in conjunction with the Vacuum Test Chamber, as seen in Figure 47. Various commercial fog nozzles could be installed and surveyed relatively quickly at controlled supply pressures. Details of the set-up and operation of the LDV are given in Appendix D.

Figure 47. Traversing LDV system set on the vacuum test chamber

B. LDV SURVEYS

Using the LDV and the vacuum chamber, the velocity field of the Hago 'mini-mist' nozzles could be determined. Initially, a 1-gph nozzle was used, and then surveys were conducted using a 4-gph nozzle. The 1-gph nozzle was not of primary interest but was used first because the lower flow rate would not empty the oil reservoir as quickly and therefore give longer times to complete surveys. When the 4-gph nozzle was used, more oil was added to the oil tank. Both nozzles were operated at oil supply gauge pressures of 77, 85 and 96 psi. The temperature of the oil when the data were taken was 95 degrees Fahrenheit. The chamber pressure for all tests reported was under 100 microns. The measurements of the velocity distributions were taken at one half inch and one inch from the exit of the nozzle. Since the wand was installed to direct the oil spray

into the bottom of the PVC T-section (to keep oil away from the windows), the centerline of the jet was pointing downwards at 25 deg to the vertical. The LDV traversed across the jet in a horizontal (x) direction. The two components of velocity given by the LDV system were Vel 1 (in the y, vertically downwards direction) and Vel 2 (in the x, horizontal direction). The LDV software output the velocity magnitude (V) from the two components, and the angle to the x-axis (θ). As can be seen in Figure 48, the flow angle with respect to the axis of the nozzle (φ) is given by $\varphi = \theta - 25$.

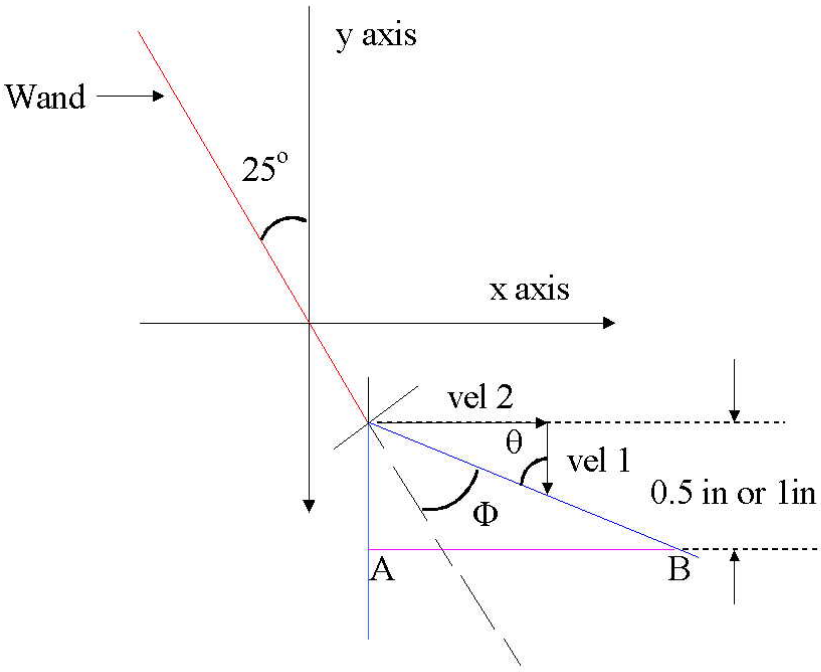

Figure 48. Nozzle flow orientation and traverse planes

C. RESULTS

1. 1-gph Mini-Mist Nozzle

The 1-gph nozzle was installed and the flow pressure was raised to 77 psig. It can be seen in the resulting flow photograph in Figure 49 that the nozzle, at that flow pressure, was not producing a mist. (Other 1-gph nozzles were subsequently mounted in turn to verify that this pattern was typical of 1-gph jets used with Marcol 5 oil) Tests to determine the velocity field were nevertheless continued since the nozzles had been used in spin tests, and the spray pattern shown in Figure 49 would have occurred.

Figure 49. 1-gph mini-mist nozzle at 77 psig

Two separate tests (A & B) were conducted to survey at distances of one half inch and one inch from the nozzle exit. The results of the four surveys at 77 psig are shown plotted in Figure 50. The starting and ending width of the pattern varied somewhat. The change in starting and ending points might indicate that the vacuum chamber moved slightly when the tank was refilled or the windows were cleaned, as well as the effect of the changing the distance of the survey plane from the nozzle. The flow pattern was expected to be a cone which was hollow in the middle, but the measured pattern for the 1-gph nozzle at 77 psig did not have a hollow center. It was likely that the non-hollow pattern was due to the nozzle not producing a mist. The average velocity for all four surveys was 23.91 m/s. The average velocity for the .5A survey was 20.75 m/s. For the .5B survey, the average velocity was 24.74 m/s. For the 1A survey the average velocity was 24.84 m/s, and for the 1B survey, the average velocity was 25.30 m/s. Thus the velocity was not changing significantly with distance from the nozzle. This would be expected since the oil droplets were moving in a vacuum.

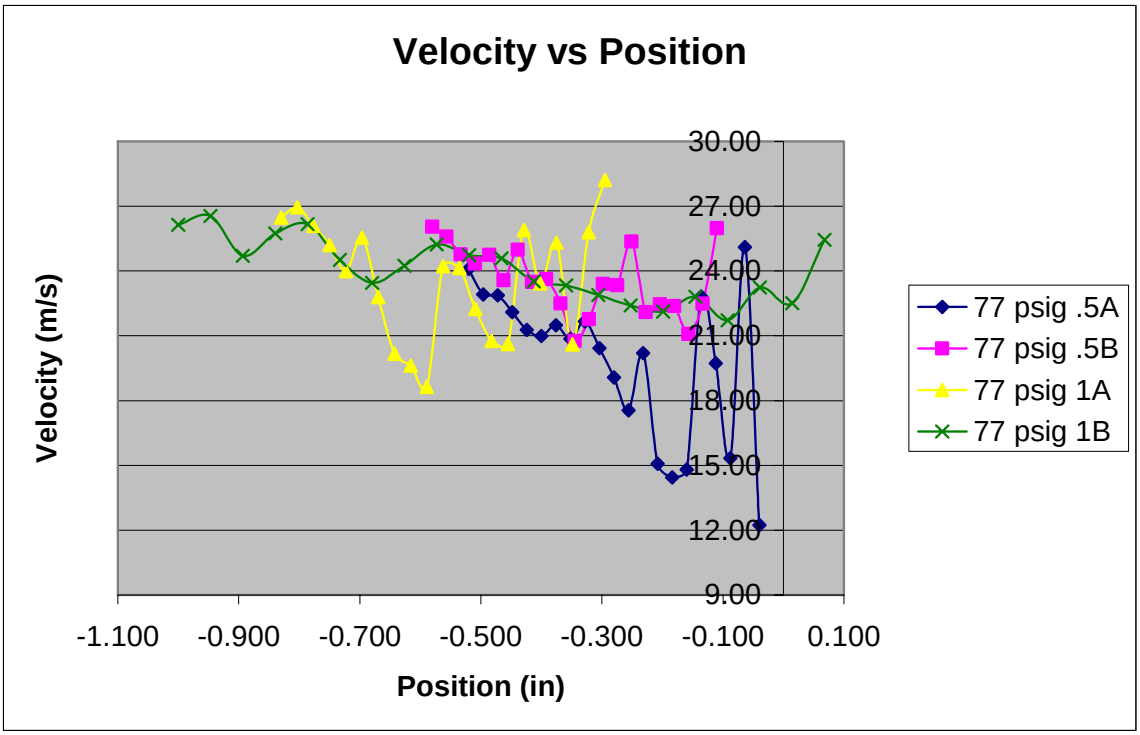

Figure 50. Surveys of 1-gph mini-mist nozzle flow field at 77 psig

Figure 51. 1-gph mini-mist nozzle at 85 psig

The 1-gph nozzle flow at a pressure of 85 psig is shown in Figure 51. Again, the nozzle did not produce a mist at this pressure. The results of the four surveys at this pressure are shown plotted in Figure 52. The oil flow pattern did not show evidence of being hollow in the middle. The starting and ending points of the pattern changed, for the same reasons as for the 77 psig surveys. The widths of the oil pattern were however about the same. The average velocity for all four surveys was 25.55 m/s. The average velocity for the .5A survey was 22.46 m/s. For the .5B survey, the average velocity was 27.35 m/s. For the 1A survey, the average velocity was 26.08 m/s, and for the 1B survey, the average velocity was 26.31 m/s. Thus the velocity was not changing significantly with distance from the nozzle; however, the average velocity at 85 psig was higher than that at 77 psig, as might be expected.

The 1-gph nozzle flow field at a pressure of 96 psig is shown in Figure 53. The nozzle did not produce a mist at this pressure. The results for the four surveys at this pressure are shown plotted in Figure 54. The pattern showed no evidence of being hollow. The starting and ending points of the pattern changed, but the widths of the pattern were about the same, for the same reasons as at the lower pressures.

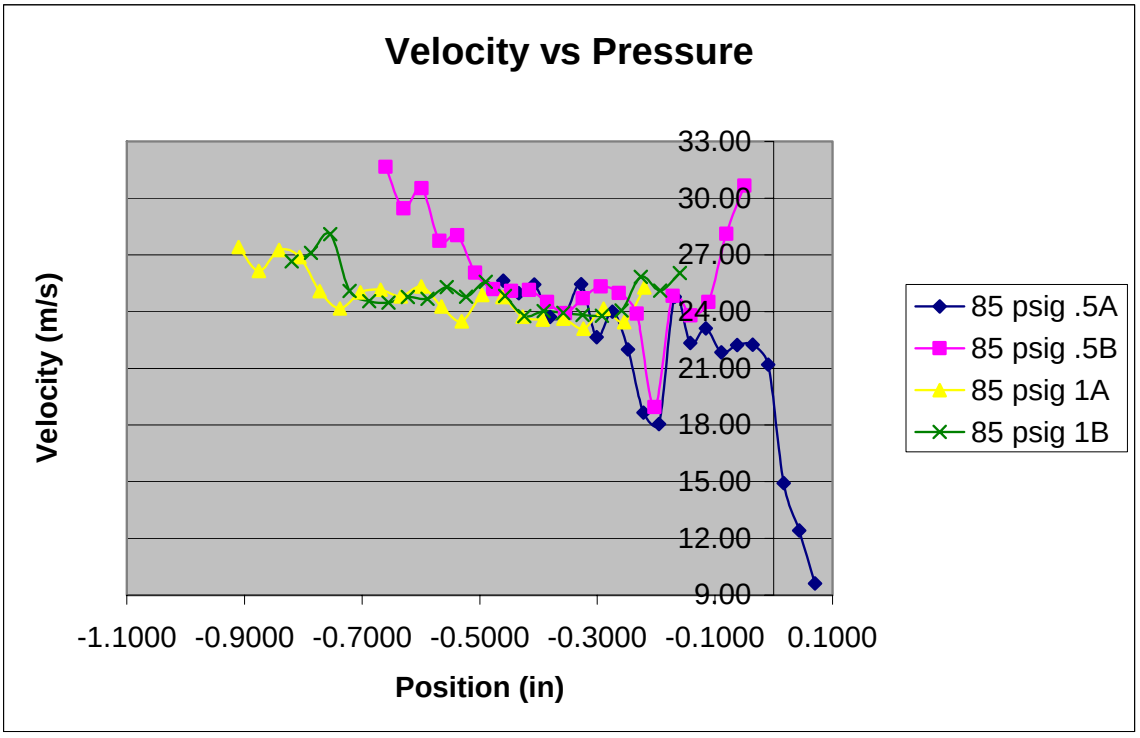

Figure 52. Surveys of 1-gph mini-mist nozzle flow field at 85 psig

Figure 53. 1-gph mini-mist nozzle at 96 psig

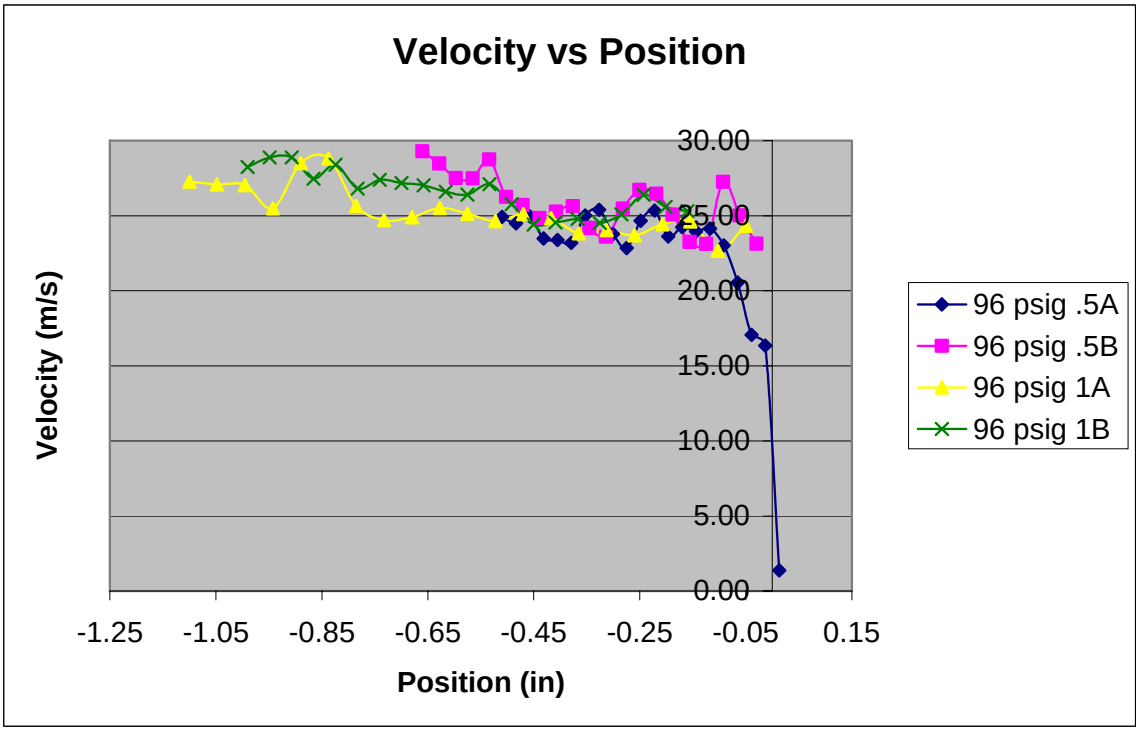

Figure 54. Surveys of 1-gph mini-mist nozzle flow field at 96 psig

The average velocity for all four surveys was 26.21 m/s. The average velocity for the .5A survey was 22.46 m/s. For the .5B survey, the average velocity was 27.35 m/s. For the 1A survey, the average was 26.08 m/s, and for the 1B survey, the average was 26.31 m/s. Thus the velocity was not changing significantly with distance from the nozzle. The average velocity at 96 psig was higher than at 85 psig, which was higher than at 77 psig, as would be expected.

2. 4-gph Mini-Mist Nozzle

The surveys of the 4-gph nozzle flow field were conducted similarly to those of 1-gph nozzle. Unfortunately, one channel of the LDV failed so that only one component of the velocity was obtained. The velocities at 77 psig were measured at twenty points as was done with the 1-gph nozzle. Fewer data points were taken at 85 psig and 96 psig, but the velocity was taken as the average of four velocity samples taken at each point. While not complete, the data did give information as to what the oil mist was doing.

Figure 55. 4-gph mini-mist nozzle at 77 psig

The 4-gph nozzle at a pressure of 77 psig is shown in Figure 55. The 4-gph nozzle did produce a mist at this pressure. Results for the vertical component of velocity at the two survey distances are shown in Figure 56.

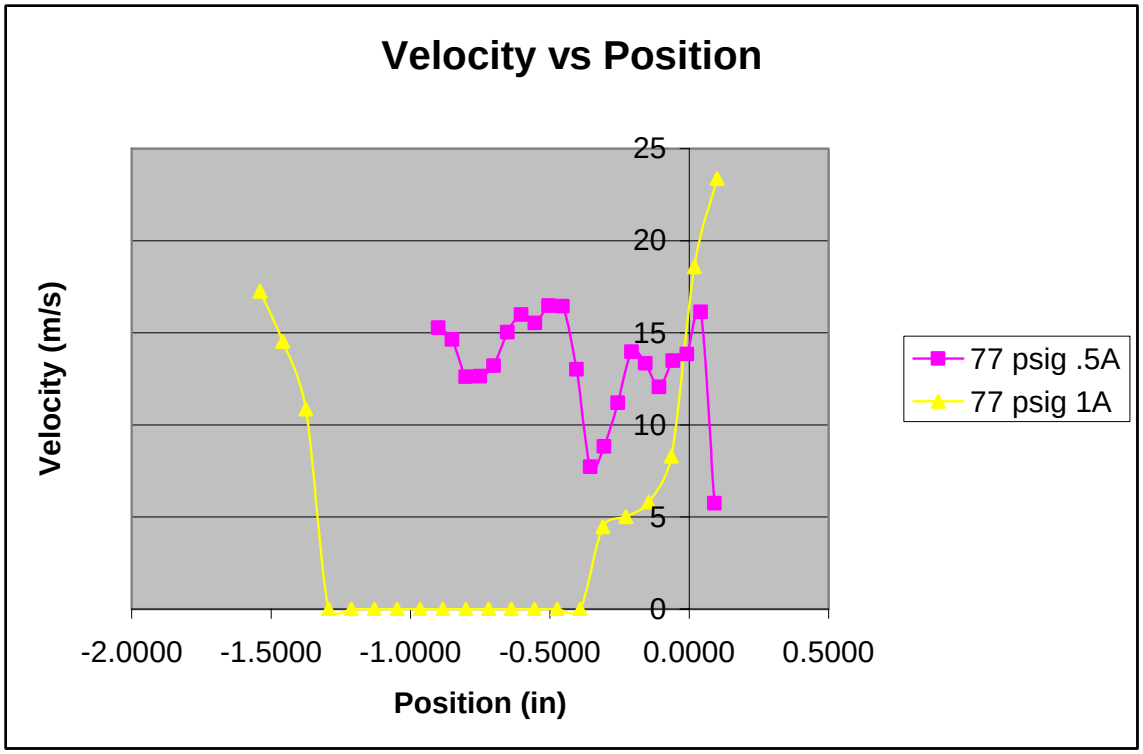

Figure 56. Surveys of 4-gph mini-mist nozzle flow field at 77 psig

The 4-gph nozzle flow pattern was found to be hollow in the middle and the hollow area was wider at the one inch distance. The difference in the overall widths at the two distances from the nozzle is more noticeable. The average velocity for the .5A run was 13.86 m/s. Due to the hollow area in the flow, an average velocity for the one inch distance was not calculated. More data points needed to be taken where there was an oil mist, but the plot showed that the maximum velocity was at the edge, and that it decreased toward the center.

The 4-gph nozzle at a flow pressure of 85 psig is shown in Figure 57. The nozzle did produce a mist at this pressure. The surveys at the two distances are shown in Figure 58. The difference in the widths at half inch and one inch from the nozzle is noticeable. The average velocity for the .5A run was 18.04 m/s. This was higher than the average velocity for the .5A run at 77 psig, as would be expected. The .5A run at 85 psig did not show evidence of the pattern being hollow in the middle, but the 1A run did show that the pattern was hollow. More data points were needed to get a useful average velocity.

Again, the plot showed that the maximum velocity was at the edge of the oil mist and that the velocity decreased toward the center of the oil mist.

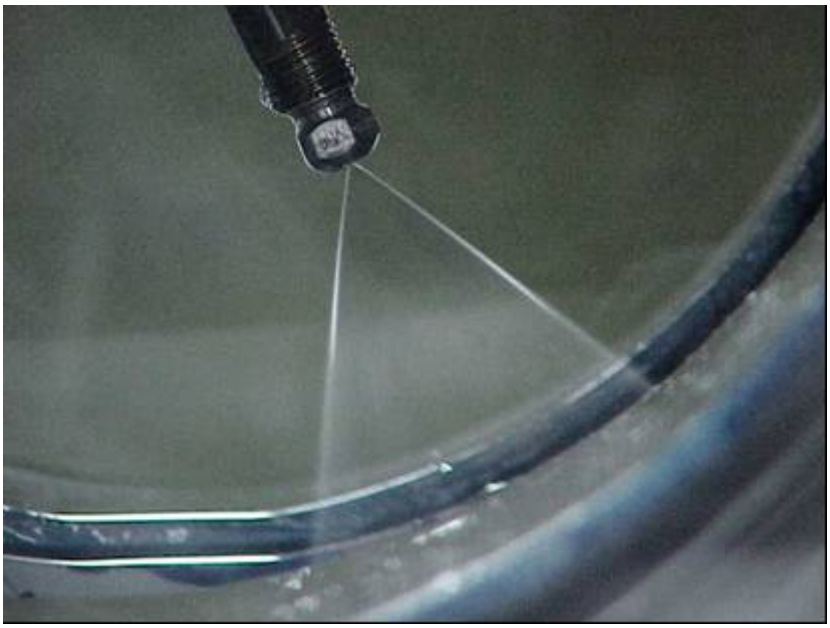

Figure 57. 4-gph mini-mist nozzle at 85 psig

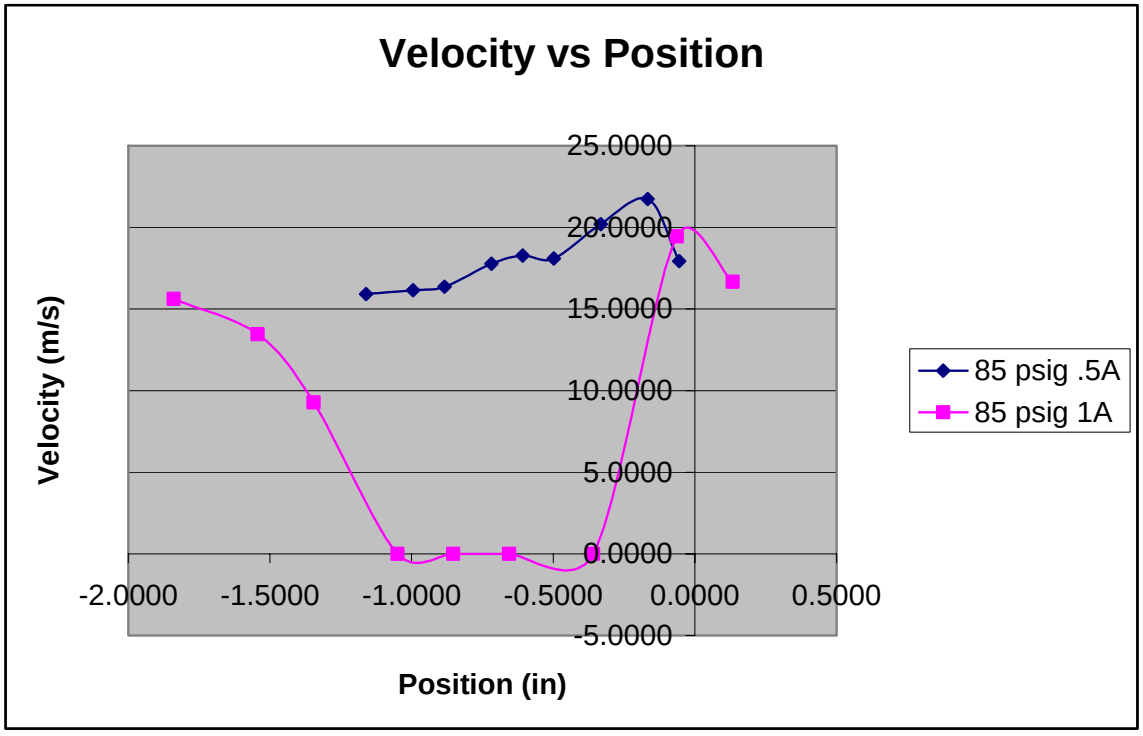

Figure 58. Survey of 4-gph mini-mist nozzle flow field at 85 psig

The 4-gph nozzle at a pressure of 96 psig is shown in Figure 59. The nozzle did produce a mist at this pressure. The surveys at the two distances are shown plotted in Figure 60.

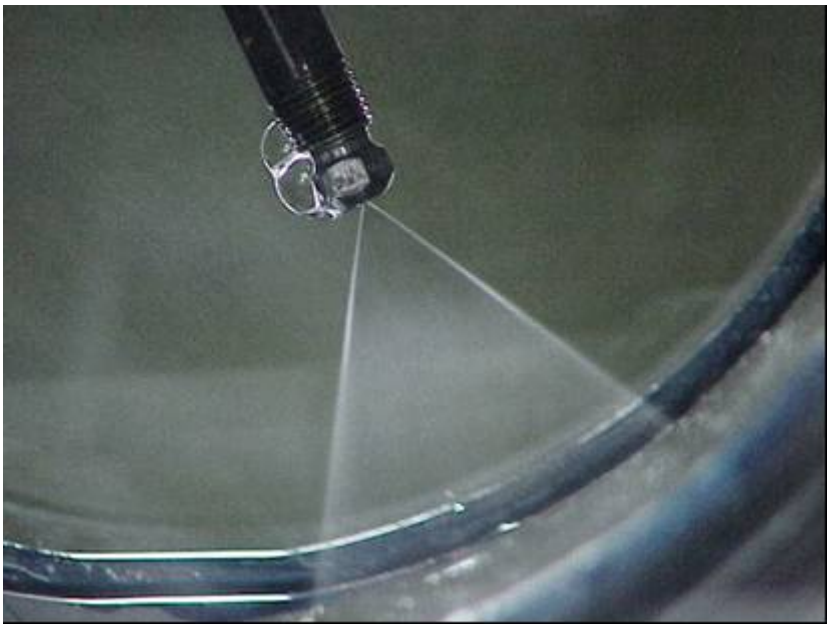

Figure 59. 4-gph mini-mist nozzle at 96 psig

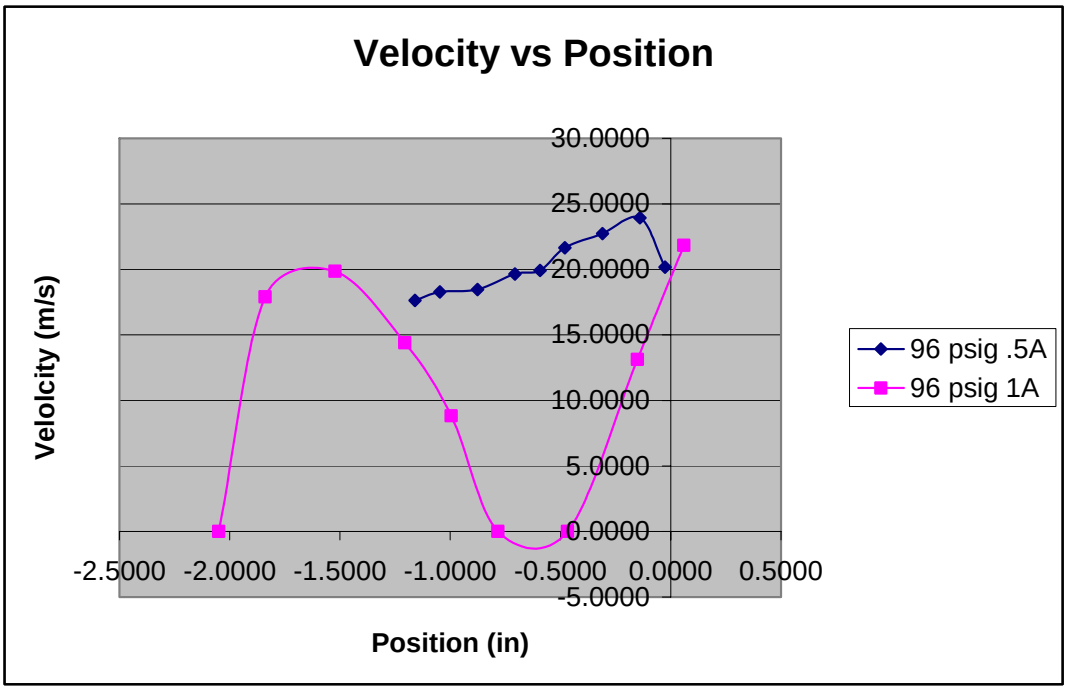

Figure 60. Surveys of 4-gph mini-mist nozzle flow field at 96 psig

The difference in the widths at one half inch and at one inch from the nozzle is noticeable. The average velocity for the .5A run was 20.27 m/s. This was higher than the average velocity for the .5A run at 85 psig, which was higher than at 77 psig, which was to be expected. The .5A run at 96 psig did not show evidence of being hollow in the middle, but the 1A run did show that the pattern was hollow. More data points were needed to get a useful average velocity. As at the previous two pressures, the velocity was maximum at the edge and decreased toward the center.

V. CONCLUSIONS AND RECOMMENDATIONS

The vacuum test chamber allowed nozzles to be tested quickly to determine whether the spray patterns were suitable for use in high cycle fatigue tests. Such tests had shown that discrete jets could, when positioned properly, generate high blade resonant excitation amplitudes in vacuum spin tests; but to avoid attendant erosion, smaller diameter jets needed to be examined. The chamber was used successfully both to evaluate prototype designs of nozzles with multiple small discrete jets, and to view the spray patterns produced by commercially available mist nozzles. Mist nozzles had not produced high excitation amplitudes in NPS spin tests, but erosion was not thought to be an issue if such nozzles were used. The spray pattern from mist nozzles was needed in order to facilitate the design of more effective excitation arrangements.

The multiple, small jet concept was first demonstrated using bundled alumina insulators with 0.005 inch diameter holes. The concept worked, but the holes were too close together, so pairs of jets coalesced. The jets were also not positioned along a single line. Small diameter stainless steel tubing was used successfully to build a prototype multiple discrete jet nozzle. However, the machine shop time required to manufacture 50 such nozzles (each with eight jets) was unacceptable. Two companies used lasers to drill small holes to fabricate prototype nozzles. But in both cases the holes were irregularly shaped rather than circular. The laser-drilled nozzles generated oil-jets, which were not parallel to each other, but sometimes the jets crossed or merged. The nozzles were cleaned and smaller filters were added, but the spray patterns remained erratic. Therefore, though laser drilling was cost effective, it did not produce nozzles that were suitable for use in high cycle fatigue tests.

Vermont Tool & Molding Company was contracted to produce nozzles by mechanically micro-drilling. The prototypes met the design requirements, that the eight discrete jets, from 0.005 inch diameter holes, were in a single line and were emitted perpendicular to the face of the nozzle. Keeping the nozzles clean as they were being used was found to be important. It was concluded that the drilled face should not even be

touched, since any trace deposit was shown to potentially change the spray pattern. An order for 50 similar nozzles was completed and delivered.

Mist nozzles that had been used at NPS and at the Navy's facility at NAWC-AD Patuxent River, MD, were tested and photographs were taken of their spray patterns. It was determined that 1-gph mini-mist nozzle did not create an oil mist at any supply pressure up to 120 psig. The 2-gph mini-mist nozzle created an oil mist only at flow pressures greater than 50 psig. The 4-gph mini-mist nozzle created an oil mist starting at low pressures. (Since the use of a higher viscosity oil in early tests produced no fog at any pressure in these three nozzles, the production of the mist appears to depend on the Reynolds number being high enough). The 6-gph standard nozzle created an oil mist, but the oil contained streaks of liquid at all flow pressures. The nozzles, when misting, could be used in high cycle fatigue tests, but the velocity of the drops needed to be established in order to calculate excitation forces.

The LDV system, set up on the vacuum test chamber, was used successfully to make measurements of the velocity of droplets from the mist nozzles. The 1-gph and the 4-gph nozzles were measured. Since the 1-gph did not mist properly, the velocity data showed that there was no hollow center to the cone of oil. The velocities were in the range 25-30 m/sec. The 4-gph nozzle results showed that the photographed cone was hollow as expected from the manufacturer's literature. The velocity of the droplets was about 20 m/sec. The measurements were sufficient to give the approximate droplet velocity within the mist for design purposes. More experiments are needed to determine the area of the cone mist, so that the oil 'impact pattern' can be defined in designing an HCF spin test, for any rotor speed, for any given oil pressure.

The vacuum test chamber should be adjusted so that the wand is vertical. This will allow velocity data to be taken in surveys that are normal to the axis of the oil mist. Velocity measurements should also be recorded starting and ending fully outside the area of the cone, so that the cone dimensions can be correlated empirically. The 4-gph nozzle produced the most consistent behavior in that it generated a (clear) mist at almost all oil

pressures, so future experiments should be initially concentrated of this nozzle. Once a set of complete profiles is obtained at different pressures, an analytic representation can be attempted.

Finally, blade excitation tests need to be conducted in the spin pit using the micro-drilled discrete jet nozzles to establish whether they can be used in a continuous HCF test without causing erosion.

THIS PAGE INTENTIONALLY LEFT BLANK

APPENDIX A. OIL-NOZZLE VACUUM TEST CHAMBER

A.1 DESCRIPTION

A schematic of the apparatus is shown in Figure 61.

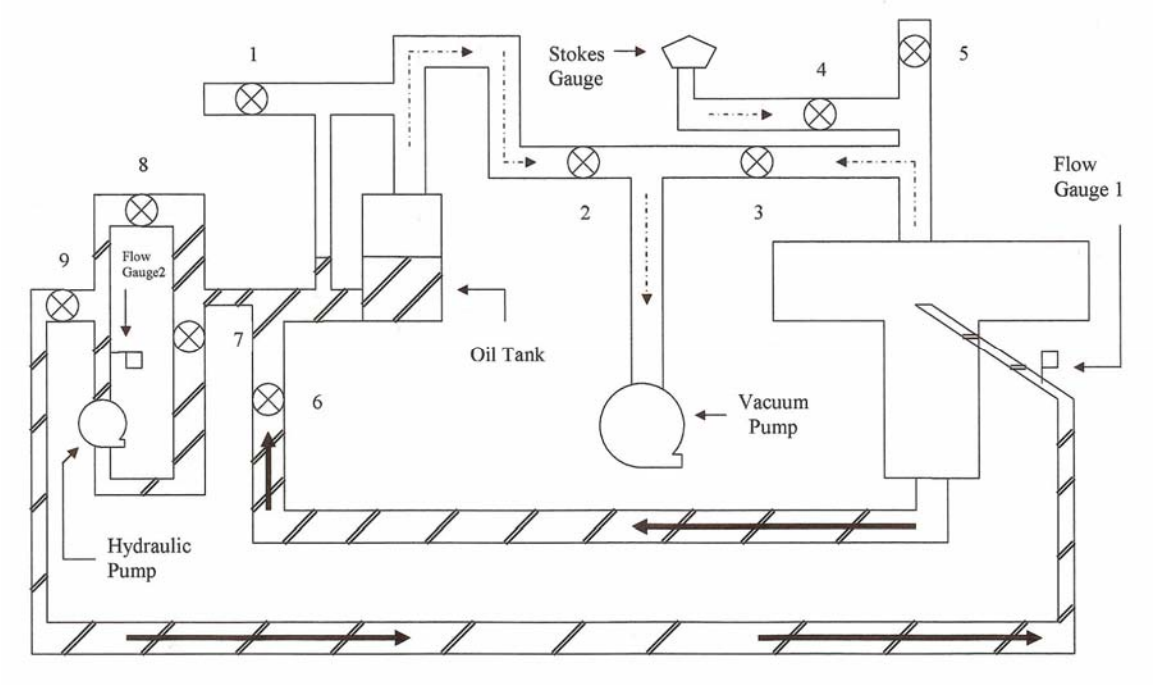

Figure 61. Schematic diagram of the test apparatus

The oil nozzle test apparatus consisted of a ten-inch diameter T-section, an oil reservoir, a hydraulic pump, a vacuum pump, and associated piping and valves. Plexiglas windows were held between flanges at opposite ends of the horizontal section of the T. The hydraulic pump (Baldor Electric motor Catalog Number L5023A, shown in Figure 62) was used to pump the oil into the nozzle. A ball valve was used to throttle the flow to increase or decrease the pressure of the flow to the nozzle. The valve, having a yellow handle and labeled valve 8 in Figure 61, is shown in Figure 63. The red handle valve in Figure A.3 is Valve 9 in Figure 61. When valve 9 was opened, it allowed oil to flow to the nozzle. A pressure gauge in the line outside the T-section (shown in Figure 64) was used to read the oil pressure as Valve 8 was adjusted to throttle the flow. A second pressure gauge in the line from the hydraulic pump, as shown in Figure 65, was used to read pressure produced by the pump.

Figure 62. Baldor Electric Motor (Catalog number L53023A)

Figure 63. Valve 8 (Yellow handle) and Valve 9 (Red handle)

Figure 64. Flow gauge 1

Figure 65. Valve 9 and Flow gauge 2

Gauge 2 was monitored to make sure the oil pressure was limited to within the capacity of the PVC piping (~300 psia). It was also used to monitor the flow into the nozzles. Both gauges showed similar pressures, differing by no more than 5 psi at higher oil flow rates.

The vacuum pump (Welch Duo-seal Vacuum Pump Model 1397 shown in Figure 66) was used to hold a near-vacuum in the T-section of the apparatus. The vacuum pump could also be used to create a vacuum in the oil reservoir.

Figure 66. Welch Duo Seal vacuum pump Model 1397

The oil reservoir, shown in Figure 67, stored and supplied the oil used during the testing. Creating a vacuum in the oil tank allowed the oil injected into the T-section to be transferred back to the tank quickly. Adjusting the valves to open the T-section to the atmosphere, with the oil tank pumped to a vacuum, the oil from the bottom of the T-section was driven into the oil tank in a matter of minutes. The near-vacuum pressure inside the T-section or the oil tank was read using the Stokes-MacLeod Gage shown in Figure 68. The pressure inside the tank could get as low as 100 microns in about 5 minutes. Occasionally, the vacuum pump was able to maintain the vacuum at about 50 microns.

Plexiglas windows were held between flanges at the two (horizontal) ends of the T-section. O-rings in the faces of the flanges were used to seal against vacuum. Following experiments using different lighting arrangements, the left side was covered with a white sheet as shown in Figure 69. The diffuse background lighting resulted in the best pictures of the oil- nozzle flows. The right side window was used to observe and photograph the flow, as show in Figure 70.

Figure 67. Oil tank

Figure 68. Stokes-MacLeod gauge

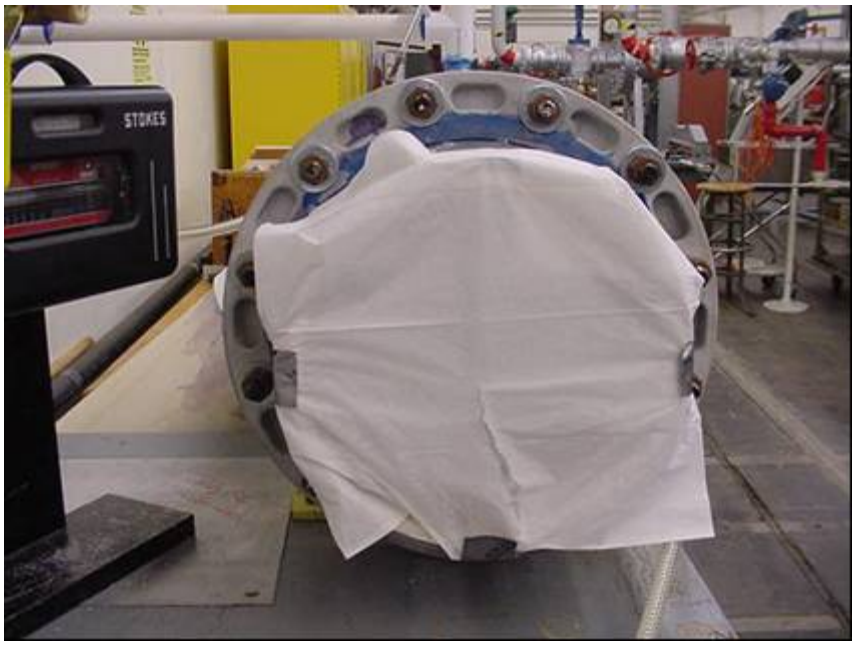

Figure 69. Left-side with white sheet

The digital camera in Figure 70 was used to take pictures of the spray patterns at different flow pressures. The camera sat on wooden blocks to ensure that the photographs were taken from the same angle, distance and height. This ensured consistency as different nozzles were tested. The Plexiglas windows could be removed for cleaning since oil could splatter and contaminate the windows.

The nozzle to be tested was attached to the end of a copper 'wand', which slipped through a Swagelok fitting in the side of the T-section, as can be seen in Figure 64. The complete wand is shown in Figure 71 and the section inside the chamber is shown enlarged in Figure 72.

The fitting could be unscrewed from the T-section to allow the nozzle to be changed. To prevent the oil nozzles from clogging, two filters were installed in series. A 3-micron filter was attached to the wand upstream of the pressure gauge as shown in Figure 4. A 5-micron filter was attached to the end of the wand, upstream of the nozzle. Keeping the oil clean was extremely important in order to prevent the small gaps in the mist nozzles from clogging or causing the small discrete jets to not exit perpendicular to the nozzle surface. If holes in the nozzles were found to be contaminated, the nozzle was removed from the wand and cleaned using pressurized nitrogen to blow out contaminant

particles. After cleaning, the nozzle was carefully re-attached to the wand. The nozzle outlet surfaces were not touched, to prevent holes being re-contaminated by particles from the hands.

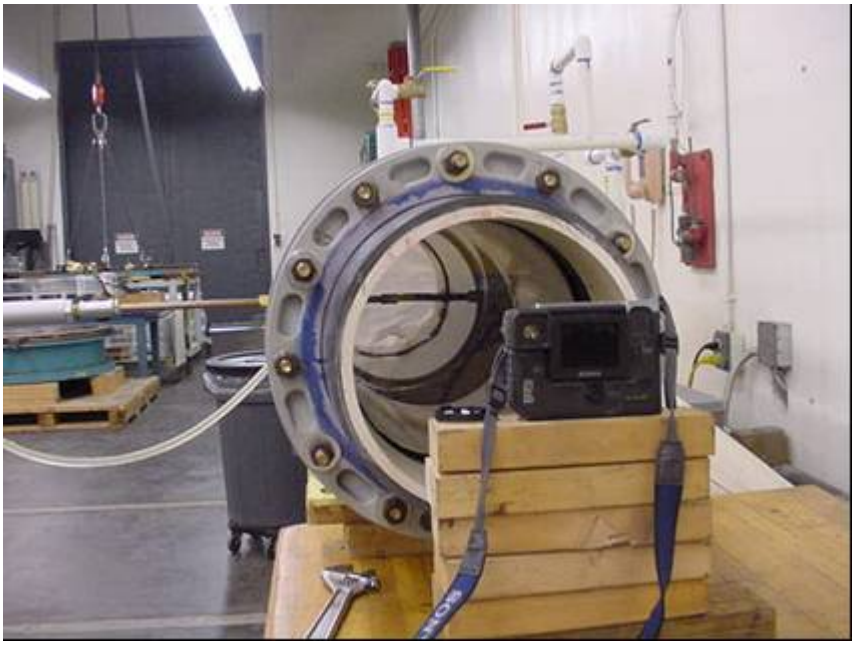

Figure 70. Right-side window with camera on wooden blocks

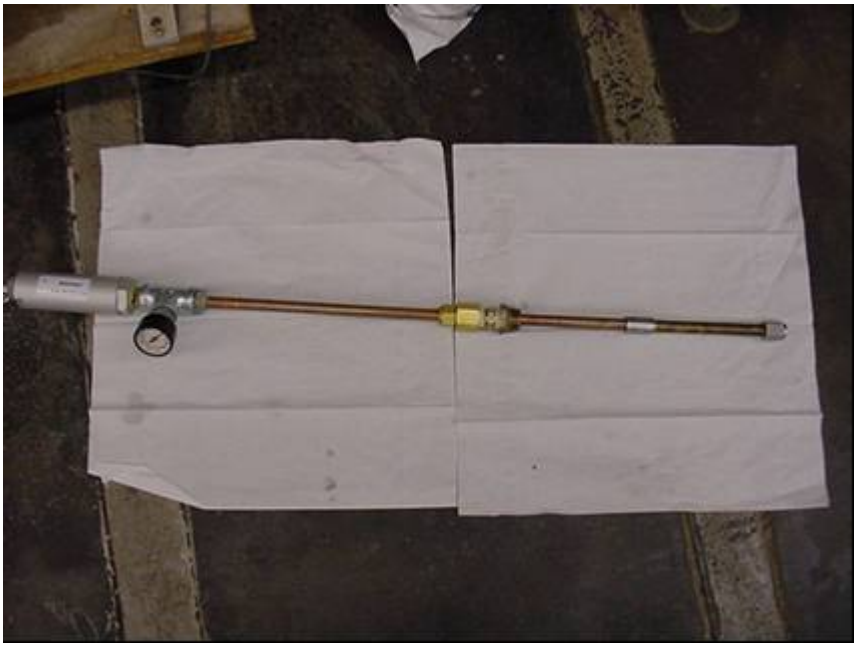

Figure 71. The wand removed from the T-section

Figure 72. Close-up of the tip of the wand

APPENDIX B. MSDS FOR MARCOL 5

A. MATERTIAL SAFETY DATA SHEETS

The following figures show the Material Safety Data Sheets (MSDS) for MARCOL 5. They are shown in Figure 73, 74, 75, 76, 77, 78, 79, and 80.

---

1. PRODUCT AND COMPANY IDENTIFICATION

PRODUCT NAME: MARCOL 5
SUPPLIER: EXXON MOBIL CORPORATION
3225 GALLOWS RD. FAIRFAX, VA
22037

24 - Hour Health and Safety Emergency (call collect): 609-737-4411 24 - Hour Transportation Emergency (Primary); CHEMTREC: 800-424-9300
(Secondary) 281-834-3296

Product and Technical Information:
Lubricants and Specialties: 800-662-4525 800-443-9966
Fuels Products: 800-947-9147
MSDS Fax on Demand: 613-228-1467
MSDS Internet Website: http://emmsds.ihssolutions.com/

---

2. COMPOSITION/INFORMATION ON INGREDIENTS

CHEMICAL NAMES AND SYNONYMS: WHITE MINERAL OIL (PETROLEUM)

GLOBALLY REPORTABLE MSDS INGREDIENTS:

None.

OTHER INGREDIENTS:

Substance Name	Approx. Wt%
WHITE MINERAL OIL (PETROLEUM) (8042-47-5)	100

See Section 8 for exposure limits (if applicable).

---

3. HAZARDS IDENTIFICATION

Under normal conditions of use, this product is not considered hazardous according to regulatory guidelines (See section 15)

EMERGENCY OVERVIEW: Clear Water White Liquid. DOT ERG No. : NA

POTENTIAL HEALTH EFFECTS: Low viscosity material - if swallowed may enter lungs and cause lung damage. Excessive exposure may result in eye, gastrointestinal, or respiratory irritation.

Figure 73. Page 1 of the MSDS for MARCOL 5

4. FIRST AID MEASURES

EYE CONTACT: Flush thoroughly with water. If irritation occurs, call a physician.
SKIN CONTACT: Wash contact areas with soap and water. Remove and clean oil soaked clothing daily and wash affected area. (See Section 16 - Injection Injury)
INHALATION: Not expected to be a problem. However, if respiratory irritation, dizziness, nausea, or unconsciousness occurs due to excessive vapor or mist exposure, seek immediate medical assistance. If breathing has stopped, assist ventilation with a mechanical device or mouth-to-mouth resuscitation.
INGESTION: Seek immediate medical attention. Do not induce vomiting. NOTE TO PHYSICIANS: Material if aspirated into the lungs may cause chemical pneumonitis.

5. FIRE-FIGHTING MEASURES

EXTINGUISHING MEDIA: Carbon dioxide, foam, dry chemical and water fog. SPECIAL FIRE FIGHTING PROCEDURES: Water or foam may cause frothing. Use water to keep fire exposed containers cool. Water spray may be used to flush spills away from exposure. Prevent runoff from fire control or dilution from entering streams, sewers, or drinking water supply.
SPECIAL PROTECTIVE EQUIPMENT: For fires in enclosed areas, fire fighters must use self-contained breathing apparatus. UNUSUAL FIRE AND EXPLOSION HAZARDS: None. COMBUSTION PRODUCTS: Fumes, smoke, carbon monoxide, sulfur oxides, aldehydes and other decomposition products, in the case of incomplete combustion.
Flash Point C(F): 154(310) (ASTM D-92).
Flammable Limits (approx.% vol. in air) - LEL: 0.9%, UEL: 7.0%
NFPA HAZARD ID: Health: 0, Flammability: 1, Reactivity: 0

6. ACCIDENTAL RELEASE MEASURES

NOTIFICATION PROCEDURES: Report spills/releases as required to appropriate authorities. U.S. Coast Guard and EPA regulations require immediate reporting of spills/releases that could reach any waterway including intermittent dry creeks. Report spill/release to Coast Guard National Response Center toll free number (800)424-8802. In case of accident or road spill notify CHEMTREC (800) 424-9300.
PROCEDURES IF MATERIAL IS RELEASED OR SPILLED:
LAND SPILL: Shut off source taking normal safety precautions. Take measures to minimize the effects on ground water. Recover by pumping or contain spilled material with sand or other suitable absorbent and remove mechanically into containers. If necessary, dispose of adsorbed residues as directed in Section 13.
WATER SPILL: Confine the spill immediately with booms. Warn other ships in the vicinity. Notify port and other relevant authorities. Remove from the surface by skimming or with suitable absorbents. If permitted by regulatory authorities the use of suitable dispersants should be considered where recommended in local oil spill procedures.
ENVIRONMENTAL PRECAUTIONS: Prevent material from entering sewers, water sources or low lying areas; advise the relevant authorities if it has, or if it contaminates soil/vegetation.
PERSONAL PRECAUTIONS: See Section 8

Figure 74. Page 2 of the MSDS for MARCOL 5

7. HANDLING AND STORAGE

HANDLING: No special precautions are necessary beyond normal good hygiene practices. See Section 8 for additional personal protection advice when handling this product.
STORAGE: Keep containers closed when not in use. Do not store in open or unlabelled containers. Store away from strong oxidizing agents and combustible materials. Do not store near heat, sparks, flame or strong oxidants.
SPECIAL PRECAUTIONS: Prevent small spills and leakages to avoid slip hazard.
EMPTY CONTAINER WARNING: Empty containers retain residue (liquid and/or vapor) and can be dangerous. DO NOT PRESSURIZE, CUT, WELD, BRAZE, SOLDER, DRILL, GRIND OR EXPOSE SUCH CONTAINERS TO HEAT, FLAME, SPARKS, STATIC ELECTRICITY, OR OTHER SOURCES OF IGNITION; THEY MAY EXPLODE AND CAUSE INJURY OR DEATH. Do not attempt to refill or clean container since residue is difficult to remove. Empty drums should be completely drained, properly bunged and promptly returned to a drum reconditioner. All containers should be disposed of in an environmentally safe manner and in accordance with governmental regulations.

8. EXPOSURE CONTROLS/PERSONAL PROTECTION

OCCUPATIONAL EXPOSURE LIMITS:

When mists/aerosols can occur, the following are recommended: 5 mg/m3 (as oil mist)- ACGIH Threshold Limit Value (TLV), 10 mg/m3 (as oil mist) - ACGIH Short Term Exposure Limit (STEL), 5 mg/m3 (as oil mist) - OSHA permissible Exposure Limit (PEL)

VENTILATION: If mists are generated, use adequate ventilation, local exhaust or enclosures to control below exposure limits.
RESPIRATORY PROTECTION: If mists are generated, and/or when ventilation is not adequate, wear approved respirator.
EYE PROTECTION: If eye contact is likely, safety glasses with side shields or chemical type goggles should be worn.
SKIN PROTECTION: If prolonged or repeated skin contact is likely, oil impervious gloves should be worn. Good personal hygiene practices should always be followed.

9. PHYSICAL AND CHEMICAL PROPERTIES

Typical physical properties are given below. forConsult Product Data Sheet specific details.

APPEARANCE: Liquid
COLOR: Clear Water White ODOR:
Odorless
ODOR THRESHOLD-ppm: NE
pH: NA
BOILING POINT C(F): NE MELTING
POINT C(F): NA FLASH POINT C(F):
154(310) FLAMMABILITY (solids): (ASTM D-92)
NE AUTO FLAMMABILITY C(F): NE
EXPLOSIVE PROPERTIES: NA
OXIDIZING PROPERTIES: NA

Figure 75. Page 3 of the MSDS for MARCOL 5

VAPOR PRESSURE-mmHg 20 C: < 0.1 VAPOR
DENSITY: > 2.0
EVAPORATION RATE: NE
RELATIVE DENSITY, 15/4 C: 0.84
SOLUBILITY IN WATER: Negligible
PARTITION COEFFICIENT: > 3.5 VISCOSITY
AT 40 C, cSt: 8.0 VISCOSITY AT 100 C,
cSt: NE
POUR POINT C(F): -9(15)
FREEZING POINT C(F): NE
VOLATILE ORGANIC COMPOUND: NE
DMSO EXTRACT, IP-346 (WT.%): <3
NA=NOT APPLICABLE NE=NOT ESTABLISHED D=DECOMPOSES

FOR FURTHER TECHNICAL INFORMATION, CONTACT YOUR MARKETING REPRESENTATIVE

---

10. STABILITY AND REACTIVITY

STABILITY (THERMAL, LIGHT, ETC.): Stable.
CONDITIONS TO AVOID: Extreme heat and high energy sources of ignition.
INCOMPATIBILITY (MATERIALS TO AVOID): Strong oxidizers.
HAZARDOUS DECOMPOSITION PRODUCTS: Product does not decompose at ambient temperatures.
HAZARDOUS POLYMERIZATION: Will not occur.

---

11. TOXICOLOGICAL DATA

---ACUTE TOXICOLOGY--

ORAL TOXICITY (RATS): Practically non-toxic (LD50: greater than 2000 mg/kg). ---Based on testing of similar products and/or the components.
DERMAL TOXICITY (RABBITS): Practically non-toxic (LD50: greater than 2000 mg/kg). ---Based on testing of similar products and/or the components.
INHALATION TOXICITY (RATS): Practically non-toxic (LC50: greater than 5 mg/l). ---Based on testing of similar products and/or the components.
EYE IRRITATION (RABBITS): Practically non-irritating. (Draize score: 0 or greater but 6 or less). ---Based on testing of similar products and/or the components.
SKIN IRRITATION (RABBITS): Practically non-irritating. (Primary Irritation Index: 0.5 or less). ---Based on testing of similar products and/or the components.

---REPRODUCTIVE TOXICOLOGY (SUMMARY)--

Oral exposure of pregnant rats to white mineral oil did not cause adverse effects in either the mothers or their offspring.

---CHRONIC TOXICOLOGY (SUMMARY)--

Repeated and/or prolonged exposure may cause irritation to the eyes or respiratory tract. Overexposure to oil mist may result in oil droplet deposition and/or granuloma formation. This product is severely solvent refined and/or severely hydrotreated. Chronic mouse skin painting studies of white mineral oils showed no evidence of carcinogenic effects.

---SENSITIZATION (SUMMARY)--

Not expected to be sensitizing based on tests of this product, components, or similar products.

Figure 76. Page 4 of the MSDS for MARCOL 5

Low viscosity white *oils* have been tested *in* sensitive rat *species* (Fischer 344) and after feeding relatively high doses (2% of diet) for 90 days, displayed some *minimal* hematological changes and liver microgranuloma. *Similar* effects were not observed to the same degree in other rodent strains or in other species. Medium to high viscosity white *oils* have been tested *in* numerous subchronic and chronic feeding, dermal, and inhalation toxicity studies. A number of test species and strains have been used, and most of the studies have shown minimal to no toxicities. *Oil* that *is* absorbed *is* retained in various tissues to some degree, but no clinical disease has been observed in the animal tests. Multiple chronic studies did not show any chronic toxicity,
cancer, or reproductive effects. Humans exposed to white *oils* with biopsy/autopsy evaluations have confirmed the presence of *oil* in tissues. with no clinical disease or long term effect on health.
Meets requirements of European Pharmacopoeia
Meets requirements of U.S. Pharmacopoeia XXIII

---

12. ECOLOGICAL INFORMATION

ENVIRONMENTAL FATE AND EFFECTS:

ECOTOXICITY: Available ectoxicity data (LLSO >1000 mg/L) indicates that adverse effects to aquatic organisms are not expected from this product.

MOBILITY: When released into the environment, adsorption to sediment and soil will be the predominant behavior.

PERSISTENCE AND DEGRADABILITY: This product is expected to be inherently biodegradable.

BIOACCUMULATIVE POTENTIAL: Bioaccumulation *is* unlikely due to the very low water solubility of this product, therefore bioavailability to aquatic organisms is minimal.

---

13. DISPOSAL CONSIDERATIONS

WASTE DISPOSAL: Product *is* suitable for burning *in* an enclosed, controlled burner for fuel value. Such burning may be limited pursuant to the Resource Conservation and Recovery Act. In addition, the product is suitable for processing by an approved recycling facility or can be disposed of at an appropriate government waste disposal facility. Use of these methods *is* subject to user compliance with applicable laws and regulations and consideration of product characteristics at time of disposal.

RCRA INFORMATION: The unused product, in our opinion, is not specifically listed by the EPA as a. hazardous waste (40 CFR, Part 261D), nor *is* it formulated to contain materials which are listed hazardous wastes. It does not exhibit the hazardous characteristics of ignitability, corrosivity, or reactivity. The unused product *is* not formulated with substances covered by the Toxicity Characteristic Leaching Procedure (TCLP). However, used product may be regulated.

---

14. TRANSPORT INFORMATION

Figure 77. Page 5 of the MSDS for MARCOL 5

USA DOT: NOT REGULATED BY USA DOT.

RID/ADR: NOT REGULATED BY RID/ADR.

IMO: NOT REGULATED BY IMO.

IATA: NOT REGULATED BY IATA.

STATIC ACCUMULATOR (50 picosiemens or less): YES

---

15. REGULATORY INFORMATION

US OSHA HAZARD COMMUNICATION STANDARD: Product assessed in accordance with OSHA 29 CFR 1910.1200 and determined not to be hazardous.

EU Labeling: Product is not dangerous as defined by the European Union Dangerous Substances/Preparations Directives.

Symbol: Not applicable.

Risk Phrase(s): Not applicable.

Safety Phrase(s): S62.
If swallowed, do not induce vomiting: seek medical advice immediately and show this container or label.

Governmental Inventory Status: All components comply with TSCA and METI.

U.S. Superfund Amendments and Reauthorization Act (SARA) Title III:
This product contains no "EXTREMELY HAZARDOUS SUBSTANCES".

SARA (311/312) REPORTABLE HAZARD CATEGORIES: None.

This product contains no chemicals subject to the supplier notification requirements of SARA (313) toxic release program.

THIS PRODUCT MEETS THE REQUIREMENTS OF FDA REGULATIONS(S): 172.878
178.3620(a)

The following product ingredients are cited on the lists below:

CHEMICAL NAME	CAS NUMBER	LIST CITATIONS

*** NO REPORTABLE INGREDIENTS ***

--- REGULATORY LISTS SEARCHED --

1=ACGIH ALL	6=IARC 1	11=TSCA 4	16=CA P65 CARC	21=LA	RTK
2=ACGIH A1	7=IARC 2A	12=TSCA 5a2	17=CA P65 REPRO	22=MI	293
3=ACGIH A2	8=IARC 2B	13=TSCA 5e	18=CA RTK	23=MN	RTK
4=NTP CARC	9=OSHA CARC	14=TSCA 6	19=FL RTK	24=NJ	RTK
5=NTP SUS	10=OSHA Z	15=TSCA 12b	20=IL RTK	25=PA RTK	
				26=RI RTK	

Code key: CARC=Carcinogeni SUS=Suspected Carcinogeni REPRO=Reproductive

Figure 78. Page 6 of the MSDS for MARCOL 5

16. OTHER INFORMATION

USE: MULTI-PURPOSE MINERAL OIL

NOTE: PRODUCTS OF EXXON MOBIL CORPORATION AND ITS AFFILIATED COMPANIES ARE NOT FORMULATED TO CONTAIN PCBS.

Health studies have shown that many hydrocarbons pose potential human health risks which may vary from person to person. Information provided on this MSDS reflects intended use. This product should not be used for other applications. In any case, the following advice should be considered:

INJECTION INJURY WARNING: If product is injected into or under the skin, or into any part of the body, regardless of the appearance of the wound or its size, the individual should be evaluated immediately by a physician as a surgical emergency. Even though initial symptoms from high pressure injection may be minimal or absent, early surgical treatment within the first few hours may significantly reduce the Ultimate extent of injury.

Precautionary Label Text:

WARNING!

LOW VISCOSITY MATERIAL-IF SWALLOWED, MAY BE ASPIRATED AND CAN CAUSE SERIOUS OR FATAL LUNG DAMAGE. EXCESSIVE EXPOSURE MAY RESULT IN EYE, GASTROINTESTINAL, OR RESPIRATORY IRRITATION.

FIRST AID: In case of contact, wash skin with soap and water. Remove contaminated clothing. Call a physician if irritation persists. Wash or dispose of contaminated clothing. If swallowed, seek immediate medical attention. Do not induce vomiting. Only induce vomiting at the instruction of a physician.

For industrial use only. Not intended or suitable for use in or around a household or dwelling.

Refer to product Material Safety Data Sheet for further safety and health information.

****

For Internal Use Only: MHC: 0* 0* 0* 0* 0*, MPPEC: A, TRN: 7332901-00, CMCS97: 97P849, REQ: PS+C, SAFE USE: L
EHS Approval Date: 13AUG2002

****

Information given herein is offered in good faith as accurate, but without guarantee. Conditions of use and suitability of the product for particular uses are beyond our control; all risks of use of the product are therefore assumed by the user and WE EXPRESSLY DISCLAIM ALL WARRANTIES OF EVERY KIND AND NATURE, INCLUDING WARRANTIES OF MERCHANTABILITY AND FITNESS FOR A PARTICULAR PURPOSE IN RESPECT TO THE USE OR SUITABILITY OF THE PRODUCT. Nothing is intended as a recommendation for uses which infringe valid patents or as extending

Figure 79. Page 7 of the MSDS for MARCOL 5

license under valid patents. Appropriate warnings and safe handling procedures should be provided to handlers and users. Alteration of this document is strictly prohibited. Except to the extent required by law, republication or retransmission of this document, in whole or in part, is not permitted. Exxon Mobil Corporation and its affiliated companies assume no responsibility for accuracy of information unless the document is the most current available from an official Exxon Mobil distribution system. Exxon Mobil Corporation and its affiliated companies neither represent nor warrant that the format, content or product formulas contained in this document comply with the laws of any other country except the United States of America.

Prepared by: Exxon Mobil Oil Corporation
Environmental Health and Safety Department, Clinton, USA

Figure 80. Page 8 of the MSDS for MARCOL 5

APPENDIX C. DIAGRAM OF THE SWAGELOK PIPE CAP

A. DIAGRAM

Figure 81 shows the diagram sent to companies to see if the could produce a prototype nozzle.

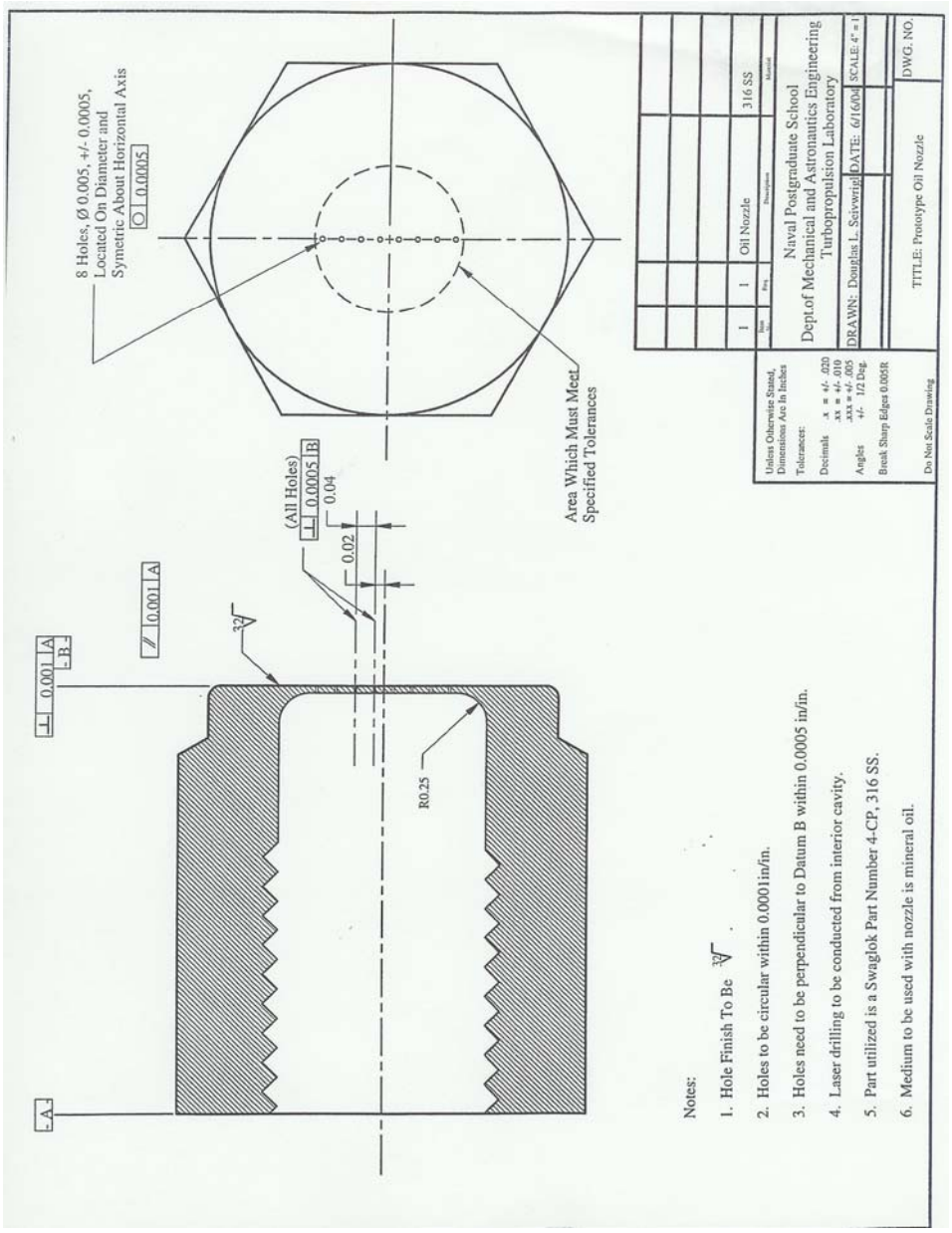

Figure 81. Diagram of the Swagelok pipe cap with required specifications

THIS PAGE INTENTIONALLY LEFT BLANK

APPENDIX D. LASER DOPPLER VELOCIMETRY APPARATUS

A schematic of the vacuum chamber and the Laser traverse system is shown in Figure 82.

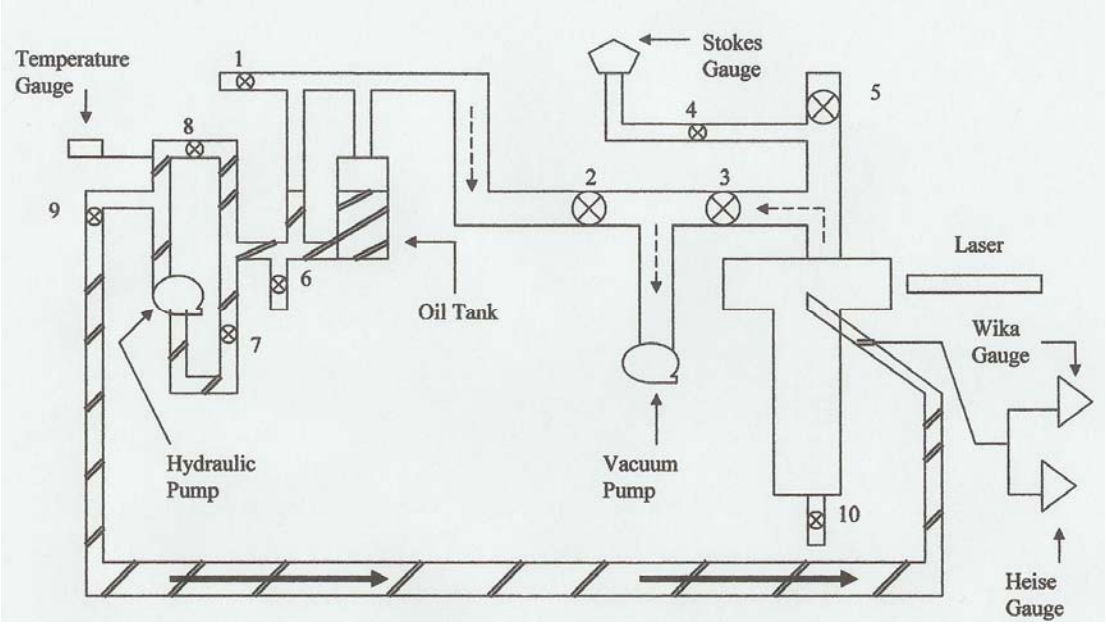

Figure 82. Schematic diagram of vacuum chamber and LDV

Information on the optics and automation of the LDV system can be found in References 23, 24, and 25. The operation of the vacuum chamber can be found in Appendix A. The laser can be traversed in the x, y, or z-direction by a transverse mechanism as shown in Figure 83. The position of the laser can be read on the output box as shown in Figure 84. The position can be changed using a hand held device as shown in Figure 85. The Z-direction was constant throughout the experiment once it was determined to be in the center of the mist. The movement in the Y-direction was set at two locations, either at half inch or one inch from the nozzle exit. The measurements were taken at equal distances along the x-axis. Figure 86 shows the laser along the x-axis within the mist of a 1-gph mini-mist nozzle in the vacuum chamber. The LDV system is attached to a computer. A computer program interprets the signals from detectors that received pulses of back-scattered light from the lasers, and outputs particle velocity. The green laser

Figure 83. LDV transverse mechanism

Figure 84. X, Y, and Z display console

Figure 85. Hand held device used to move LDV

Figure 86. Laser in use with in a mist from a 1-gph mini-mist nozzle

gives the vertical component of velocity and the blue laser gives the horizontal component of the velocity. The green laser velocity component is Velocity 1, and the blue laser velocity component is Velocity 2. The computer program gives real time values for the velocities. The wand can be adjusted to be farther into the chamber to prevent oil droplets from appearing on the windows as shown in Figure 87. Droplets on the windows, especially the window on the laser side will degrade the reflected light signal back to the computer. The vacuum chamber was made so that the windows can be taken off to be cleaned and put back quickly.

Figure 87. Vacuum chamber with adjustable wand

APPENDIX E. LDV VELOCITY DATA TABLES

Date	3-Feb-05						
Nozzle	1 gph						
Pressure (psig)	77						
Pressure (micron)	125						
Temperature (F)	95						
Z position (in)	0.0000						
Y position (in)	-0.5000						
X position (in)	**Vel 1**	**Vel 2**	**Magnitude**	**Theta**	**vel 1**	**vel 2**	**magnitude**
-0.5200	15.40	18.53	24.09	50.27	14.22	18.89	23.64
-0.4960	14.72	17.57	22.92	50.04			
-0.4720	14.29	17.87	22.88	51.35			
-0.4480	15.33	15.91	22.09	46.06			
-0.4240	15.41	14.66	21.27	43.57			
-0.4000	16.49	13.00	21.00	38.25	15.42	12.59	19.91
-0.3760	17.49	12.49	21.49	35.53			
-0.3520	17.02	12.05	20.85	35.30			
-0.3280	18.63	11.06	21.67	30.70			
-0.3040	18.14	9.39	20.43	27.37			
-0.2800	18.34	5.23	19.07	15.92	19.91	8.56	21.67
-0.2560	16.86	4.89	17.55	16.17			
-0.2320	18.93	7.06	20.20	20.45			
-0.2080	14.73	3.19	15.07	12.22			
-0.1840	14.25	2.38	14.45	9.48			
-0.1600	14.68	1.95	14.81	7.57	15.88	2.51	16.08
-0.1360	22.50	3.79	22.82	9.56			
-0.1120	19.60	2.26	19.73	6.58			
-0.0880	15.27	1.45	15.34	5.42			
-0.0640	25.01	-2.23	25.11	-5.10			
-0.0400	12.12	-1.75	12.25	-8.22	12.03	1.24	12.09
		AVG	20.75				

Table 1. 1-gph mini-mist nozzle: Run A with the flow pressure at 77 psig and 0.5 inch from the nozzle exit.

Date	14-Feb-05						
Nozzle	1 gph						
Pressure (psig)	77						
Pressure (micron)	70						
Temperature (F)	95						
Z position (in)	0.0000						
Y position (in)	-0.5000						
X position (in)	**Vel 1**	**Vel 2**	**Magnitude**	**Theta**	**vel 1**	**vel 2**	**magnitude**
-0.5800	16.19	20.41	26.05	51.58	16.22	20.62	26.23
-0.5565	16.26	19.76	25.59	50.55			
-0.5330	16.31	18.64	24.77	48.81			
-0.5095	16.47	17.93	24.35	47.43			
-0.4860	17.66	17.34	24.75	44.48			
-0.4625	17.99	15.23	23.57	40.25	18.78	14.96	24.01
-0.4390	16.85	18.45	24.99	47.60			
-0.4155	19.75	12.72	23.49	32.78			
-0.3920	19.51	13.32	23.62	34.32			
-0.3685	18.42	12.92	22.50	35.05			
-0.3450	17.06	11.84	20.77	34.76	17.23	11.37	20.64
-0.3215	19.05	10.54	21.77	28.95			
-0.2980	20.94	10.45	23.40	26.52			
-0.2745	20.40	11.36	23.35	29.11			
-0.2510	20.51	14.92	25.36	36.03			
-0.2275	18.85	11.52	22.09	31.43	18.40	10.42	21.15
-0.2040	20.45	9.28	22.46	24.41			
-0.1805	20.94	7.90	22.38	20.67			
-0.1570	20.03	6.58	21.08	18.19			
-0.1335	22.45	1.13	22.48	2.88			
-0.1100	25.89	2.10	25.98	4.64	26.44	7.85	27.58
		AVG	24.74				

Table 2. 1-gph mini-mist nozzle: Run B with the flow pressure at 77 psig and 0.5 inch from the nozzle exit.

Date	8-Feb-05						
Nozzle	1gph						
Pressure (psig)	77						
Pressure (micron)	300						
Temperature (F)	95						
Z position (in)	0.0000						
Y position (in)	-1.0000						
X position (in)	**Vel 1**	**Vel 2**	**Magnitude**	**Theta**	**vel 1**	**vel 2**	**magnitude**
-0.8300	17.06	20.25	26.48	49.89	16.17	20.34	25.98
-0.8033	19.21	18.90	26.95	44.53			
-0.7765	18.86	18.03	26.09	43.71			
-0.7498	19.13	16.41	25.20	40.62			
-0.7230	19.00	14.64	23.99	37.62			
-0.6963	20.83	14.80	25.55	35.39	16.48	12.56	20.72
-0.6695	19.37	12.01	22.79	31.80			
-0.6428	18.74	7.47	20.17	21.73			
-0.6160	18.69	5.96	19.62	17.69			
-0.5892	17.54	6.32	18.64	19.82			
-0.5625	22.17	9.76	24.22	23.76	21.79	9.49	23.77
-0.5357	22.25	9.37	24.14	22.84			
-0.5090	20.33	9.02	22.24	23.93			
-0.4822	18.87	8.66	20.76	24.65			
-0.4555	19.08	7.82	20.62	22.29			
-0.4287	20.59	15.72	25.90	37.36	19.71	6.36	20.71
-0.4020	21.66	8.91	23.42	22.36			
-0.3752	22.09	12.35	25.31	29.21			
-0.3485	19.65	6.20	20.60	17.51			
-0.3217	25.53	3.66	25.79	8.16			
-0.2950	28.10	2.57	28.22	5.23	20.51	3.92	20.88
		AVG	24.84				

Table 3. 1-gph mini-mist nozzle: Run A with the flow pressure at 77 psig and 1 inch from the nozzle exit.

Date	10-Feb-05						
Nozzle	1 gph						
Pressure (psig)	77						
Pressure (micron)	100						
Temperature (F)	95						
Z position (in)	0.0000						
Y position (in)	-1.0000						
X position (in)	**Vel 1**	**Vel 2**	**Magnitude**	**Theta**	**vel 1**	**vel 2**	**magnitude**
-1.0000	17.62	19.32	26.15	47.63	17.20	19.59	26.07
-0.9466	18.01	19.50	26.54	47.27			
-0.8932	17.14	17.79	24.70	46.07			
-0.8398	19.77	16.47	25.73	39.80			
-0.7864	21.17	15.39	26.17	36.02			
-0.7330	19.84	14.40	24.52	35.97	19.74	14.27	24.36
-0.6796	19.48	13.07	23.46	33.86			
-0.6262	19.85	13.93	24.25	35.06			
-0.5728	20.84	14.22	25.23	34.31			
-0.5194	21.06	12.96	24.73	31.61			
-0.4660	21.63	11.67	24.58	28.35	21.45	10.33	23.81
-0.4126	21.67	9.13	23.51	22.85			
-0.3592	22.36	6.64	23.33	16.54			
-0.3058	21.94	6.50	22.88	16.50			
-0.2524	21.91	4.65	22.40	11.98			
-0.1990	21.88	3.25	22.12	8.45	23.49	2.11	23.58
-0.1456	22.75	1.52	22.80	3.82			
-0.0922	21.66	1.66	21.72	4.38			
-0.0388	23.19	1.38	23.23	3.41	22.89	2.13	22.99
0.0146	22.50	0.77	22.51	1.96			
0.0680	25.35	-2.10	25.44	-4.74			0.00
		AVG	25.30				

Table 4. 1-gph mini-mist nozzle: Run B with the flow pressure at 77 psig and 1 inch from the nozzle exit.

Date	3-Feb-05						
Nozzle	1 gph						
Pressure (psig)	85						
Pressure (micron)	125						
Temperature (F)	95						
Z position (in)	0.0000						
Y position (in)	-0.5000						
X position (in)	**Vel 1**	**Vel 2**	**Magnitude**	**Theta**	**vel 1**	**vel 2**	**magnitude**
-0.4600	17.97	18.28	25.63	45.49	17.25	18.92	25.60
-0.4335	18.35	16.93	24.97	42.70			
-0.4070	19.78	15.99	25.43	38.95			
-0.3805	18.13	15.29	23.72	40.14			
-0.3540	18.96	14.57	23.91	37.54			
-0.3275	21.34	13.86	25.45	33.00	18.39	13.02	22.53
-0.3010	18.96	12.40	22.65	33.19			
-0.2745	20.16	13.01	23.99	32.84			
-0.2480	18.72	11.54	21.99	31.65			
-0.2215	15.42	10.50	18.66	34.25			
-0.1950	15.13	9.86	18.06	33.09	18.63	8.12	20.32
-0.1685	22.27	10.86	24.78	26.00			
-0.1420	20.96	7.74	22.34	20.27			
-0.1155	21.47	8.55	23.11	21.71			
-0.0890	20.97	6.12	21.84	16.27			
-0.0625	21.59	5.32	22.24	13.84	21.00	6.12	21.87
-0.0360	21.70	4.89	22.24	12.70			
-0.0095	21.11	1.80	21.19	4.87			
0.0170	14.87	1.21	14.92	4.65			
0.0435	12.37	1.12	12.42	5.17			
0.0700	9.54	1.23	9.62	7.35	15.65	0.38	15.65
		AVG	22.46				

Table 5. 1-gph mini-mist nozzle: Run A with the flow pressure at 85 psig and 0.5 inch from the nozzle exit.

Date	15-Feb-05						
Nozzle	1 gph						
Pressure (psig)	85						
Pressure (micron)	60						
Temperature (F)	95						
Z position (in)	0.0000						
Y position (in)	-0.5000						
X position (in)	**Vel 1**	**Vel 2**	**Magnitude**	**Theta**	**vel 1**	**vel 2**	**magnitude**
-0.6600	19.21	25.16	31.66	52.64	19.26	24.95	31.52
-0.6295	18.34	23.06	29.46	51.50			
-0.5990	19.96	23.09	30.52	49.16			
-0.5685	17.87	21.22	27.74	49.90			
-0.5380	19.72	19.92	28.03	45.29			
-0.5075	18.68	18.15	26.05	44.18	19.09	17.99	26.23
-0.4770	19.71	15.68	25.19	38.50			
-0.4465	20.35	14.69	25.10	35.82			
-0.4160	20.38	14.71	25.13	35.82			
-0.3855	20.00	14.17	24.51	35.32			
-0.3550	20.57	12.20	23.92	30.67	20.75	11.20	23.58
-0.3245	21.95	11.35	24.71	27.34			
-0.2940	23.45	9.55	25.32	22.16			
-0.2635	23.33	8.92	24.98	20.92			
-0.2330	23.05	6.25	23.88	15.17			
-0.2025	18.07	5.71	18.95	17.54	17.53	8.11	19.32
-0.1720	24.37	4.74	24.83	11.01			
-0.1415	22.94	6.34	23.80	15.45			
-0.1110	23.91	5.40	24.51	12.73			
-0.0805	27.34	6.52	28.11	13.41			
-0.0500	30.62	1.62	30.66	3.03	23.12	1.86	23.19
		AVG	27.35				

Table 6. 1-gph mini-mist nozzle: Run B with the flow pressure at 85 psig and 0.5 inch from the nozzle exit.

Date	8-Feb-05						
Nozzle	1 gph						
Pressure (psig)	85						
Pressure (micron)	60						
Temperature (F)	95						
Z position (in)	0.0000						
Y position (in)	-1.0000						
X position (in)	**Vel 1**	**Vel 2**	**Magnitude**	**Theta**	**vel 1**	**vel 2**	**magnitude**
-0.9100	18.89	19.86	27.41	46.43	18.51	19.73	27.05
-0.8755	17.83	19.12	26.14	47.00			
-0.8410	20.73	17.71	27.26	40.51			
-0.8065	22.35	14.96	26.89	33.80			
-0.7720	21.50	12.91	25.08	30.98			
-0.7375	19.77	13.89	24.16	35.09	19.71	13.77	24.04
-0.7030	20.60	14.18	25.01	34.54			
-0.6685	21.67	12.76	25.15	30.49			
-0.6340	21.70	12.00	24.80	28.94			
-0.5995	22.39	11.83	25.32	27.85			
-0.5650	21.57	11.14	24.28	27.31	21.76	10.10	23.99
-0.5305	21.43	9.62	23.49	24.18			
-0.4960	23.09	9.25	24.87	21.83			
-0.4615	23.37	8.21	24.77	19.36			
-0.4270	22.66	7.04	23.73	17.26			
-0.3925	22.69	6.39	23.57	15.73	22.69	4.50	23.13
-0.3580	23.11	4.90	23.62	11.97			
-0.3235	22.61	4.75	23.10	11.86			
-0.2890	23.83	3.93	24.15	9.36	23.95	0.71	23.96
-0.2545	23.24	3.07	23.44	7.53			
-0.2200	25.25	1.30	25.28	2.95	0.00	0.00	0.00
		AVG	26.08				

Table 7. 1-gph mini-mist nozzle: Run A with the flow pressure at 85 psig and 1 inch from the nozzle exit.

Date	11-Feb-05						
Nozzle	1 gph						
Pressure (psig)	85						
Pressure (micron)	100						
Temperature (F)	95						
Z position (in)	0.0000						
Y position (in)	-1.0000						
X position (in)	**Vel 1**	**Vel 2**	**Magnitude**	**Theta**	**vel 1**	**vel 2**	**magnitude**
-0.8200	18.89	18.80	26.65	44.86	19.47	18.93	27.16
-0.7870	19.56	18.77	27.11	43.82			
-0.7540	22.89	16.29	28.09	35.44			
-0.7210	20.77	14.07	25.09	34.11			
-0.6880	20.02	14.22	24.56	35.39			
-0.6550	19.74	14.47	24.48	36.24	20.19	13.25	24.15
-0.6220	20.19	14.35	24.77	35.40			
-0.5890	20.03	14.42	24.68	35.75			
-0.5560	20.56	14.73	25.29	35.62			
-0.5230	20.18	14.40	24.79	35.51			
-0.4900	21.58	13.71	25.57	32.43	21.19	12.64	24.67
-0.4570	21.84	11.82	24.83	28.42			
-0.4240	21.77	9.54	23.77	23.66			
-0.3910	22.52	8.38	24.03	20.41			
-0.3580	22.71	7.54	23.93	18.37			
-0.3250	22.72	7.18	23.83	17.54	22.29	7.71	23.59
-0.2920	22.97	6.17	23.78	15.04			
-0.2590	23.59	4.74	24.06	11.36			
-0.2260	25.48	4.25	25.83	9.47			
-0.1930	24.83	3.77	25.11	8.63			
-0.1600	25.94	2.27	26.04	5.00	22.69	2.02	22.78
		AVG	26.31				

Table 8. 1-gph mini-mist nozzle: Run B with the flow pressure at 85 psig and 1 inch from the nozzle exit.

Date	4-Feb-05						
Nozzle	1 gph						
Pressure (psig)	96						
Pressure (micron)	150						
Temperature (F)	95						
Z position (in)	0.0000						
Y position (in)	-0.5000						
X position (in)	**Vel 1**	**Vel 2**	**Magnitude**	**Theta**	**vel 1**	**vel 2**	**magnitude**
-0.51	11.19	22.25	24.91	63.30	14.01	17.90	22.73
-0.48385	15.91	18.62	24.49	49.49			
-0.4577	17.17	18.12	24.96	46.54			
-0.43155	16.10	17.10	23.49	46.73			
-0.4054	16.83	16.24	23.39	43.98			
-0.37925	18.06	14.55	23.19	38.86	17.90	14.36	22.95
-0.3531	20.01	15.01	25.01	36.87			
-0.32695	19.84	15.84	25.39	38.60			
-0.3008	20.01	12.85	23.78	32.71			
-0.27465	19.49	11.90	22.84	31.41			
-0.2485	21.02	12.89	24.66	31.52	22.78	10.28	24.99
-0.22235	22.73	11.21	25.34	26.25			
-0.1962	21.77	9.17	23.62	22.84			
-0.17005	22.67	8.56	24.23	20.69			
-0.1439	22.64	7.77	23.94	18.94			
-0.11775	23.38	6.03	24.15	14.46	23.42	3.01	23.61
-0.0916	22.57	4.56	23.03	11.42			
-0.06545	20.30	3.11	20.54	8.71			
-0.0393	17.00	1.40	17.06	4.71			
-0.01315	16.29	1.22	16.34	4.28			
0.013	0.25	1.35	1.37	79.51	1.64	1.65	2.33
		AVG	23.29				

Table 9. 1-gph mini-mist nozzle: Run A with the flow pressure at 96 psig and 0.5 inch from the nozzle exit.

Date	15-Feb-05						
Nozzle	1 gph						
Pressure (psig)	96						
Pressure (micron)	60						
Temperature (F)	95						
Z position (in)	0.0000						
Y position (in)	-0.5000						
X position (in)	**Vel 1**	**Vel 2**	**Magnitude**	**Theta**	**vel 1**	**vel 2**	**magnitude**
-0.6600	19.04	22.24	29.28	49.43	19.24	21.23	28.65
-0.6285	19.05	21.17	28.48	48.02			
-0.5970	19.16	19.73	27.50	45.84			
-0.5655	19.96	18.90	27.49	43.44			
-0.5340	21.30	19.29	28.74	42.17			
-0.5025	22.50	13.53	26.25	31.02	22.66	13.78	26.52
-0.4710	21.15	14.60	25.70	34.62			
-0.4395	20.27	14.34	24.83	35.28			
-0.4080	21.49	13.26	25.25	31.68			
-0.3765	22.35	12.55	25.63	29.32			
-0.3450	21.63	10.82	24.19	26.58	21.60	10.81	24.15
-0.3135	22.05	8.42	23.60	20.90			
-0.2820	23.10	10.72	25.47	24.89			
-0.2505	23.72	12.30	26.72	27.41			
-0.2190	24.48	10.05	26.46	22.32			
-0.1875	24.45	5.56	25.07	12.81	24.23	5.75	24.90
-0.1560	21.78	8.16	23.26	20.54			
-0.1245	21.70	7.95	23.11	20.12			
-0.0930	26.69	5.55	27.26	11.75			
-0.0615	24.60	4.49	25.01	10.34			
-0.0300	22.98	-2.69	23.14	-6.68	24.27	0.89	24.29
		AVG	27.12				

Table 10. 1-gph mist-mini nozzle: Run B with the flow pressure at 96 psig and 0.5 inch from the nozzle exit.

Date	8-Feb-05						
Nozzle	1 gph						
Pressure (psig)	96						
Pressure (micron)	60						
Temperature (F)	95						
Z position (in)	0.0000						
Y position (in)	-1.0000						
X position (in)	**Vel 1**	**Vel 2**	**Magnitude**	**Theta**	**vel 1**	**vel 2**	**magnitude**
-1.1000	18.47	20.06	27.27	47.36	17.59	20.52	27.03
-1.0475	18.84	19.46	27.09	45.93			
-0.9950	19.75	18.48	27.05	43.10			
-0.9425	19.64	16.25	25.49	39.60			
-0.8900	22.74	17.21	28.52	37.12			
-0.8375	24.21	15.65	28.83	32.88	21.52	15.87	26.74
-0.7850	20.97	14.76	25.64	35.14			
-0.7325	20.95	13.10	24.71	32.02			
-0.6800	21.65	12.28	24.89	29.56			
-0.6275	21.96	12.98	25.51	30.59			
-0.5750	22.03	12.08	25.12	28.74	22.13	12.55	25.44
-0.5225	22.00	11.08	24.63	26.73			
-0.4700	22.94	10.18	25.10	23.93			
-0.4175	23.09	9.15	24.84	21.62			
-0.3650	22.55	7.72	23.83	18.90			
-0.3125	23.29	5.97	24.04	14.38	24.11	6.97	25.10
-0.2600	23.26	4.56	23.70	11.09			
-0.2075	24.22	3.12	24.42	7.34			
-0.1550	24.46	2.84	24.62	6.62	23.98	0.89	24.00
-0.1025	22.56	2.26	22.67	5.72			
-0.0500	24.30	1.28	24.33	3.02	0.00	0.00	0.00
		AVG	26.62				

Table 11. 1-gph mini-mist nozzle: Run A with the flow pressure at 96 psig and 1 inch from the nozzle exit.

Date	14-Feb-05						
Nozzle	1 gph						
Pressure (psig)	96						
Pressure (micron)	80						
Temperature (F)	95						
Z position (in)	0.0000						
Y position (in)	-1.0000						
X position (in)	**Vel 1**	**Vel 2**	**Magnitude**	**Theta**	**vel 1**	**vel 2**	**magnitude**
-0.9900	19.64	20.30	28.25	45.95	19.56	20.64	28.44
-0.9485	20.87	19.95	28.87	43.71			
-0.9070	21.59	19.18	28.88	41.62			
-0.8655	21.61	16.94	27.46	38.09			
-0.8240	23.12	16.47	28.39	35.46			
-0.7825	20.95	16.74	26.82	38.63	20.85	16.29	26.46
-0.7410	21.81	16.57	27.39	37.23			
-0.6995	22.48	15.27	27.18	34.19			
-0.6580	22.63	14.78	27.03	33.15			
-0.6165	22.98	13.40	26.60	30.25			
-0.5750	23.20	12.61	26.41	28.53	23.85	13.45	27.38
-0.5335	24.45	11.68	27.10	25.53			
-0.4920	23.21	11.20	25.77	25.76			
-0.4505	22.45	9.60	24.42	23.15			
-0.4090	22.96	8.67	24.54	20.69			
-0.3675	23.82	6.80	24.77	15.93	23.72	6.21	24.52
-0.3260	23.97	5.06	24.50	11.92			
-0.2845	24.82	3.71	25.10	8.50			
-0.2430	26.19	3.18	26.38	6.92			
-0.2015	25.45	2.70	25.59	6.06			
-0.1600	25.29	-0.84	25.30	-1.90	24.96	1.10	24.98
		AVG	27.84				

Table 12. 1-gph mini-mist nozzle: Run B with the flow pressure at 96 psig and 1 inch from the nozzle exit.

Date	19-Feb-05
Nozzle	4 gph
Pressure (psig)	77
Pressure (micron)	70
Temperature (F)	95
Z position (in)	0.0000
Y position (in)	-0.5000
X position (in)	**Vel 1**
0.0900	5.75
0.0405	16.13
-0.0090	13.85
-0.0585	13.49
-0.1080	12.06
-0.1575	13.34
-0.2070	13.97
-0.2565	11.2
-0.3060	8.83
-0.3555	7.73
-0.4050	13.02
-0.4545	16.45
-0.5040	16.48
-0.5535	15.53
-0.6030	15.99
-0.6525	15.03
-0.7020	13.21
-0.7515	12.64
-0.8010	12.61
-0.8505	14.64
-0.9000	15.28
AVG	13.8615

Table 13. 4-gph mini-mist nozzle: Run A with the flow pressure at 77 psig and 0.5 inch from the nozzle exit.

Date	19-Feb-05
Nozzle	4 gph
Pressure (psig)	77
Pressure (micron)	100
Temperature (F)	95
Z position (in)	0.0000
Y position (in)	-1.0000
X position (in)	**Vel 1**
0.1000	23.38
0.0180	18.58
-0.0640	8.30
-0.1460	5.81
-0.2280	5.02
-0.3100	4.46
-0.3920	0.00
-0.4740	0.00
-0.5560	0.00
-0.6380	0.00
-0.7200	0.00
-0.8020	0.00
-0.8840	0.00
-0.9660	0.00
-1.0480	0.00
-1.1300	0.00
-1.2120	0.00
-1.2940	0.00
-1.3760	10.86
-1.4580	14.53
-1.5400	17.26

Table 14. 4-gph mini-mist nozzle: Run B with the flow pressure at 77 psig and 1 inch from the nozzle exit.

Date	20-Feb-05
Nozzle	4 gph
Pressure (psig)	85
Pressure (microns)	800
Temperature (F)	88
Z position (in)	0.0000
Y position (in)	-0.5000
X position (in)	**Vel 1**
-0.0560	17.9275
-0.1664	21.7325
-0.3320	20.1975
-0.4976	18.0925
-0.6080	18.2775
-0.7184	17.7750
-0.8840	16.3650
-0.9944	16.1475
-1.1600	15.9075
AVG	18.0469

Table 15. 4-gph mini-mist nozzle: Run A with the flow pressure at 85 psig and 0.5 inch from the nozzle exit.

Date	20-Feb-05
Nozzle	4 gph
Pressure (psig)	85
Pressure (microns)	800
Temperature (F)	88
Z position (in)	0.0000
Y position (in)	-1.0000
X position (in)	**Vel 1**
0.1340	16.6625
-0.0633	19.4575
-0.3593	0.0000
-0.6552	0.0000
-0.8525	0.0000
-1.0498	0.0000
-1.3458	9.2800
-1.5431	13.4575
-1.8390	15.6050

Table 16. 4-gph mini-mist nozzle: Run B with the flow pressure at 85 psig and 1 inch from the nozzle exit.

Date	20-Feb-05
Nozzle	4 gph
Pressure (psig)	96
Pressure (microns)	800
Temperature (F)	93
Z position (in)	0.0000
Y position (in)	-0.5000
X position (in)	**Vel 1**
-0.0260	20.1700
-0.1394	23.9425
-0.3095	22.7300
-0.4796	21.6525
-0.5930	19.9300
-0.7064	19.6575
-0.8765	18.4600
-1.0466	18.2750
-1.1600	17.6300
AVG	20.2719

Table 17. 4-gph mini-mist nozzle: Run A with the flow pressure at 96 psig and 0.5 inch form the nozzle exit.

Date	20-Feb-05
Nozzle	4 gph
Pressure (psig)	96
Pressure (microns)	800
Temperature (F)	93
Z position (in)	0.0000
Y position (in)	-1.0000
X position (in)	**Vel 1**
0.0600	21.8375
-0.1510	13.1275
-0.4675	0.0000
-0.7840	0.0000
-0.9950	8.8225
-1.2060	14.4075
-1.5225	19.8675
-1.8390	17.9125
-2.0500	0.0000

Table 18. 4-gph mini-mist nozzle: Run B with the flow pressure at 96 psig and 1 inch from the nozzle exit.

LIST OF REFERENCES

1. Shreeve, R.P., Seivwright, D.L. and Hobson, G.V., "Navy Rotor Spin Research Facility and Initial Program", Paper presented at the 4th National Turbine Engine High-Cycle Fatigue (HCF) Conference, Feb 9-11, 1999, Monterey, CA.

2. Mercadal, M., von Flotow, A. and Roesler, C., "Results of Eddy Current Excitation of Blade Vibration in a Series of Rotors", Proceedings of the 6th National Turbine Engine High-Cycle Fatigue (HCF) Conference, Jacksonville, FL, March 5-8, 2001.

3. Shreeve, R. P., Hobson, G. V., Seivwright, D. L. and Mansisidor, M. R., "Turbine Rotor Spin Tests Using Eddy-Current and Air-Jet Excitation Techniques", Proceedings of the 7th National Turbine Engine High-Cycle Fatigue (HCF) Conference, W. Palm Beach, FL, May 14-17, 2002.

4. Shreeve, R. P., Hobson, G. V., Seivwright, D. L. and Russell, S. A., "Vacuum Spin Test Experience with Eddy-Current Excitation of a Large Titanium Fan Blisk," Proceedings of the 8th National Turbine Engine High-Cycle Fatigue (HCF) Conference, Monterey, CA, April 14-16, 2003

5. Shreeve, R. P., Seivwright, D. L. and Hobson, G. V., "HCF Spin-Testing with Oil-Jet Excitation", Proceedings of the 9th National Turbine Engine High-Cycle Fatigue (HCF) Conference, Pinehurst, NC, March 16-19, 2004.

6. Shreeve, R.P., Seivwright, D.L., Hobson, G.V. and Moreno, O., "Oil-Jet Excitation in Rotor Spin Testing", Proceedings of the 10th National Turbine Engine High-Cycle Fatigue (HCF) Conference, New Orleans, LA, March 8-11, 2005.

7. Sonnichsen, H. E., "HCF Characterization and Life Measurements in Spin Pits," Paper presented at the 9th National Engine High-Cycle Fatigue (HCF) Congerence, Pinehurst, NC, March 16-19, 2004.

8. Heyman, Frank J., "Conclusions from the ASTM interlaboratory test program with liquid impact erosion facilities," Proceeding of the Fifth International Conference on Erosion by Liquid and Solid Impact: Newham College Cambridge, 3-6 September 1979.

9. Janakiram, K. S., Sasikanth, S. R., and Syamala Rao, B. C., "Liquid Jet Impact Studies with Ordinary and Cavijets," Proceedings of the Fifth Conference on Fluid Machinery, Budapest, Hungary, 15-20 September, 1975.

10. Richman, R. H, "Liquid Impact Erosion," ASM Handbook, Failure Analysis and Prevention, Volume 11 2002.

11. Heyman, Frank J., "Liquid Impingement Erosion," ASM Handbook, Volume 18, 1992.

12. Thomas, G. P., and Brunton. J. H., "Drop Impingement Erosion of Metals," Proceeding Royal Society London, Series A, Volume 314 Number 1519, 1970.

13. Stack, M. M., and Pungwiwat, N., "Slurry Erosion of Metallics, Polymers, and Ceramics: Particle Size Effects," Materials Science and Technology, London, Volume 15 Issue 3, March 1999.

14. Walton, D, Spence, M. K., and Reynolds, B. T., "The Effects of Free Stream Air Velocity on Water Droplet Size and Distribution for an Impaction Spray Nozzle," Proceeding of the Institution of Mechanical Engineers Volume 214 Part A, 2000.

15. "Cutting and Drilling." www.coherent.com.au/industrial/mat_cuttinganddrilling.htm accessed on November 17, 2004.

16. "Laser Drilling." Home.comcst.net/~laserwiz/drilling/htm accessed on November 4, 2004.

17. "Laser Welding & Cutting." www.acceleroninc.com/techdata/laser-ndyag.htm accessed on November 4, 2004.

18. "CO_2 Laser Cutting." www.acceleroninc.com/techdata/laser-co2.htm accessed on November 4, 2004.

19. "Electrical Discharge Machining and Wire EDM Capabilities." www.starkindutrial.com/precision_wire.htm accessed November 4, 2004.

20. Moser, Harry C. "When do you need EDM?" www.mmsonline.com/article/029503.html accessed on October 8, 2004.

21. "EDM Basics." www.jjjtrain.com/vms/other/edm_basics/html accessed on September 29, 2004.

22. "Electrical Discharging Machining." En.wikipedia.org/wiki/Electrical_discharging_machining accessed on September 29, 2004.

23. Elazar, Y. "A Mapping of the Viscous Flow Behavior in a Controlled Diffusion Compressor Cascade and Preliminary Evaluation of Codes for the Prediction of Stall," Thesis, Naval Postgraduate School, Monterey, CA, March 1988.

24. Murray, K. D. "Automation and Extension of LDV Measurement of Off-Design Flow in a Cascade Wind Tunnel," Thesis, Naval Postgraduate School, Monterey, CA June 1989.

25. Schnorenberg, D. G. “Investigation of the Effect of Reynolds Number on Laminar Separation Bubbles on Controlled-Diffusion Compressor Blades in Cascade,” Thesis, Naval Postgraduate School, Monterey, CA, June 1996.

THIS PAGE INTENTIONALLY LEFT BLANK

INITIAL DISTRIBUTION LIST

1. Defense Technical Information Center
   Ft. Belvoir, Virginia

2. Dudley Knox Library
   Naval Postgraduate School
   Monterey, California

3. Dr. Raymond Shreeve
   Naval Post Graduate School
   Monterey, California

4. Dr. Garth Hobson
   Naval Post Graduate School
   Monterey, California

5. Raymond Pickering
   Naval Air Systems Command (AIR 4.4)
   Patuxent River, Maryland

6. Dr. Andy von Flotow
   Hood Technology Corporation
   Hood River, Oregon